

RESEARCH ARTICLE

Changes in extreme temperature and precipitation indices: Using an innovative daily homogenized database in Israel

Yizhak Yosef^{1,2}  | Enric Aguilar³ | Pinhas Alpert¹¹Department of Geophysics, Tel-Aviv University, Tel-Aviv, Israel²Climate Department, Israel Meteorological Service, Bet-Dagan, Israel³Center on Climate Change (C3), Universitat Rovira i Virgili, Tarragona, Spain**Correspondence**

Yizhak Yosef, Department of Geophysics, Tel-Aviv University, Tel-Aviv, Israel.

Email: yizhakyosef@mail.tau.ac.il

Funding information

Israeli Science Foundation, Grant/Award Number: 1123/17

Abstract

This study examines the 1950–2017 temporal changes in climate extremes in Israel, which is located in the East Mediterranean (EM), a region which suffers from a scarcity of long and reliable datasets. It is well known that most long-term records are affected by artificial shifts most commonly caused by station relocation, instrumental modification and local environmental changes. Therefore, for the first time, a thorough homogenization (detection and correction) routine was developed and implemented in the long-term records. Consequently, a new daily adjusted dataset has been generated, including 34 temperature stations and 60 precipitation stations. Based on this comprehensive dataset, 38 extreme indices recommended by the Expert Team on Climate Change Detection and the Expert Team on Sector-specific Climate Indices have been calculated. These indices will help various sectors to plan properly mitigation actions and adaptation for climate change, in addition to facilitating future studies for the EM. The results showed highly significant changes in temperature extremes associated with warming, especially for those indices derived from the daily minimum temperature (TN, 1950–2017), whereas the maximum temperature (TX) exhibited a similar increasing magnitude of the TN ($\sim 0.55^\circ\text{C}/\text{decade}$) in the last 30 years. The warming trends, which are non-monotonic, seem to have been particularly strong since the early 1990s. The coastal area is characterized by higher heat stress during the nighttime, while mountains exhibit a strong tendency towards increasing temperatures during the noon hours. A reduction in the total precipitation amount and in the number of wet days with a tendency towards more intense wet days was found. Although all the regional trends of the precipitation indices were not statistically significant ($p \leq .05$), they showed a fine spatial coherence.

KEYWORDS

climate change, East Mediterranean, extreme indices, homogenization, Israel, precipitation, temperature, trend analysis

1 | INTRODUCTION

In recent decades, more and more research has focused on climate change in general, and extreme weather in particular, mainly due to the expected broad effects on society

and various economic sectors (e.g., agriculture, health, water and energy).

Numerous changes in extreme weather and climate have been observed since around 1950 (IPCC, 2014). According to the literature, on a global scale, it is very likely (90–100%

probability) that a decline in the number of cold days and nights has taken place, while warm days and nights have increased. Furthermore, heat waves have become more frequent in many parts of Europe, Asia and Australia. In general, it is likely (66–100%) that in land regions, heavy precipitation events have become more frequent (e.g., North America and Europe), whereas in other continents the confidence level is medium at most (IPCC, 2014). Donat *et al.* (2013) reported significant warming trends related to temperature extremes indices, mostly stronger for those based on daily TNs than for indices calculated from daily TXs based on a new global land-based gridded dataset. Additionally, a tendency towards wetter conditions for most precipitation indices was found on a global scale.

Since the previous century, a general warming tendency over the Mediterranean was found (Alpert *et al.*, 2008; Mariotti *et al.*, 2015) along with increasing temperatures at the 850-hPa pressure level for the summer over the East Mediterranean (EM; Saaroni *et al.*, 2003; Shohami *et al.*, 2011). Zhang *et al.* (2005a) reported a general warming tendency in the Middle East (ME) from 1950 to 2003. They also found a significant increase in the frequency of warm days as the 1990s drew near, while the frequency of cold days has gradually decreased significantly since the 1970s.

Ben-Gai *et al.* (1999) analysed the changes in frequency distribution patterns of the temperature during 1964–1979 versus 1980–1994 at some selected stations in Israel. They found that during the second sub-period, throughout most of the country, the mean of the TX and TN shifts towards lower temperatures in February, while in August the mean shifts towards higher temperature values. A positive minimum (0.2–0.9°C/decade) and maximum (0.3–0.7°C/decade) daily temperature trends were found in 10 different stations across Israel, most of them are significant, for the period 1964–2003 (Shohami *et al.*, 2011). In our previous study (Yosef *et al.*, 2018), we analysed the temperature trends in Israel, based on five long-term stations records, during 1950–2011, using for the first time monthly adjusted (homogenized) time series. A highly significant positive trend was found for the annual TN with 0.15°C/decade ($p = .002$), whereas the TX trend was 0.10°C/decade ($p = .051$). Furthermore, the most pronounced seasonal trends were recorded in the summer, which was characterized by significant positive trends for TX (0.15°C/decade) and TN (0.23°C/decade), while the winter exhibited no significant positive trends.

Extreme precipitation studies conducted in the Mediterranean reveal some increasing trends, such as in Italy and Spain for torrential rainfall (up to 128 mm/day). At the same time, there was an increasing trend in heavy rainfall (32–64 mm/day) in Israel and heavy to torrential rainfall in Cyprus for the period 1951–1995; however, only the trends

for Spain and Italy were found to be statistically significant (Alpert *et al.*, 2002). A later study focusing on Israel revealed a significant increase in the heavy to torrential daily rainfall in some stations, mainly over the southern coastal plain of Israel, although no significant change was observed in the annual rainfall over the period 1950/1–2003/4 (Yosef *et al.*, 2009). Kostopoulou and Jones (2005) reported positive trends in the number of days with daily precipitation above 10 mm for Italy and significant negative trends in the eastern part of the Mediterranean (mainly in the western part of Greece) for 1958–2000. In the ME, weak non-significant trends in precipitation extreme indices and lack of spatial coherence were found by Zhang *et al.* (2005a) during 1950–2003.

Very few long-term studies have been conducted on climate extremes in Israel and adjacent countries. Moreover, most research did not use a homogenized database, but rather chose to exclude the suspected time series from the analysis. The calculation of indices requires high-quality, high-frequency (daily or better), homogeneous meteorological data (Zwiers *et al.*, 2013). The latter is crucial to better estimate long-term trends, since most meteorological records are affected by a number of non-climatic factors such as station relocation, instrumentation issues (e.g., replacement, change in calibration, maintenance), screen type changes, environmental changes in the vicinity of meteorological stations and more. These factors usually have a major impact on time series, in the form of abrupt and/or gradual changes (“break-point,” BP), which compromise their validity to represent climate variability and change (Aguilar *et al.*, 2003). A previous study (Yosef *et al.*, 2018) demonstrated the influence of the homogenization procedure on the trend magnitude (and statistical significance) focusing on a few stations in Israel. The authors showed that instrumentation issues along with station relocation were responsible for more than 60% of the BPs.

The aim of this study is twofold. First, we plan to generate a long-term temperature and precipitation daily homogenized database with high spatial resolution. This unbiased analysis is crucial for understanding the EM climate change, which suffers from a scarcity of long and reliable datasets. The second goal is to examine temporal and spatial changes in long-term temperature and precipitation extreme indices based on this cutting-edge daily database that is mandatory for extreme analysis.

This paper is organized as follows: the study area, database, homogenization procedures and indices calculations are discussed in Section 2. In Section 3, we present the main results of the long- and short-term trends analysis for the temperature and precipitation extreme indices. Section 4 is dedicated to discussion and Section 5 for summary and main conclusions.

2 | STUDY AREA AND METHODOLOGY

2.1 | The study area

Israel is located in the subtropical region in the southeastern corner of the Mediterranean Sea, with a Mediterranean climate (type Csa, based on Köppen climate classification) in the northern and central parts of the country, and a semiarid (type BSh) and arid (type BWb) climate in the southern and southeastern parts. The country's climate is also affected by its complex topography: a coastal plain in the west through a mountain range that extends from north to south, via the central part of the country, and a deep depression—the Jordan—Dead Sea Valley, in the east. These features yield a large climatic diversity across a small country. Israel is typically characterized by hot and dry summers, and cold wet winters. The rainy season lasts from October to May, and within this period, the majority (two-thirds) of the annual precipitation falls in December through February. Israel's rainfall is unevenly distributed and characterized by extreme

spatial variability. In the northern parts, the average annual rainfall exceeds 900 mm and approximately 500 mm in the centre. On the other hand, rainfall isohyets may drop sharply to 200 mm when headed southward and eastward within a span of only a few kilometres. In the southern parts, annual rainfall averages are below 100 mm. All of these factors thereby facilitate exploration of various climatic types.

2.2 | Data and quality control

The database contains 24 daily temperature stations and 60 daily precipitation stations based on records from 1950 to 2017. Moreover, 14 other temperature stations were added to the homogenization stage, yet only 10 of these were included in the short-term trend analysis (1988–2017). The two maps in Figure 1 depict the geographical distributions of the temperature and precipitation stations. Additional information about their coordinates, heights and periods of record, are listed in Tables S1 and S2.

Most of the time series in this study were screened systematically by a quality control system operated by the Israel

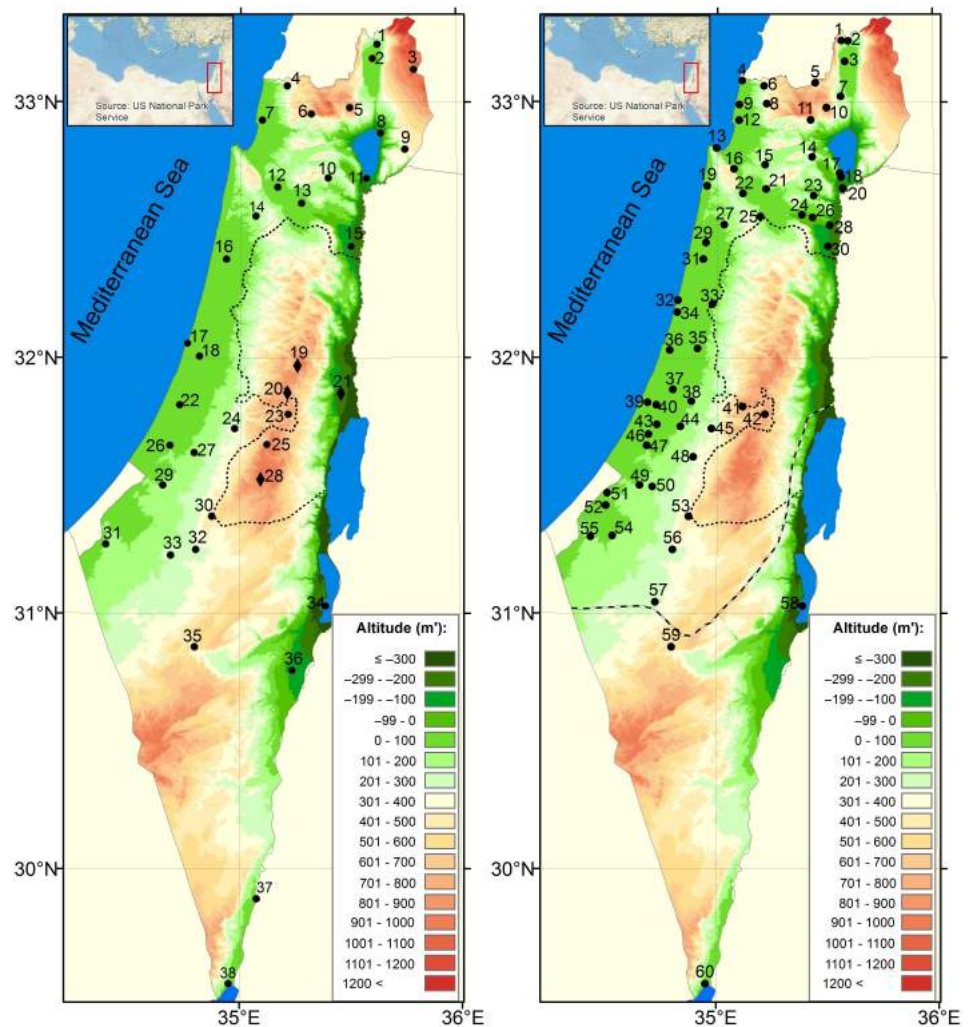


FIGURE 1 Location of the stations in this study. Left panel: Temperature stations are denoted by black circles, while black rhombi denote stations that were used only for the homogenization steps. Right panel: Precipitation stations in which dashed line denotes the averaged 100 mm isohyet over the period 1981–2010 (the arid region is to the south) [Colour figure can be viewed at wileyonlinelibrary.com]

Meteorological Service (IMS). Several short periods were verified with RCLimDex quality control software (Zhang and Yang, 2004), in addition to spatial checks that were also applied. Furthermore, the quality control tool implemented in HOMER (Mestre *et al.*, 2013) based on CLIMATOL (Guijarro, 2011) was applied to analyse outliers, histograms and boxplots for the whole dataset. The outliers detected by ACMANT (Domonkos, 2011) were examined as well. Finally, missing daily values of the adjusted temperature database were completed by linear regression based on highly correlated stations. This includes a reconstruction of 13 to 44 months going backwards to 1950 for stations number: 2, 22, 29 and 31 (using stations from the same climatological region where $r > 0.95$). The preparation of the precipitation dataset involved two major steps. The first phase was to divide the total daily rainfall amount of days that were flagged with accumulated rain amount. The second step was to fill in missing daily values by estimating the expected amount using highly correlative neighbouring stations and/or by subdivide their documented monthly value (if any) into daily amounts.

2.3 | The homogenization procedure

As mentioned earlier, most of the long meteorological records are affected by a number of non-climatic factors that usually have a major impact on the time series (comparable to climate change). Hence, the impact of these factors must be assessed and corrected (homogenized) before computing any trends, to ensure that time fluctuations in the data are only caused by variations in climate and not by any artificial factors. Therefore, a thorough homogenization scheme was developed, by implementing some state-of-the-art methods as suggested by Venema *et al.* (2012) based on a blind inter-comparison and validation study.

Our analysis was based mostly on relative homogenization methods that compare differences or examine ratios between the base station (i.e., the station to be homogenized) and a reference time series (i.e., neighbouring stations and/or an average of several highly correlated ones). A log transformation was applied to the monthly precipitation amounts. The three main methods we have implemented were as follows.

- ACMANT (Domonkos, 2011; Domonkos and Coll, 2017): The Adapted Caussinus-Mestre Algorithm for Networks of Temperature. This method is based on a bivariate detection of changes that include a penalty term (Caussinus and Mestre, 2004). ACMANT works fully automatically and uses weighted reference time series. This method uses the core of the detection and adjustment methods of the PRODIGE (step function fitting and
- analysis of variance [ANOVA] correction segments, Caussinus and Mestre, 2004).
- HOMER (Mestre *et al.*, 2013): HOMogenization software in R (HOMER) is one of the most advanced methods that includes the finest features from several leading methods like PRODIGE that uses a pairwise comparison (Caussinus and Mestre, 2004), ACMANT (Domonkos, 2011) and joint segmentation method (Picard *et al.*, 2011). HOMER includes bivariate detection for shifts in the annual means and the summer–winter differences and the minimization of the residual variance in finding the optimal adjustment terms (ANOVA). HOMER is an interactive method, which takes advantage of metadata. There are some subjective decision parts where expert intervention is required.
- CLIMATOL (Guijarro, 2011, 2018): The homogenization procedure relies on a method for estimating data at one point by means of other synchronous data from nearby stations, using a form of orthogonal regression known as reduced major axis (Leduc, 1987). After estimating the data, the Standard Normal Homogeneity Test (Alexandersson, 1986) is applied to the anomalies time series (i.e., differences between the normalized original and estimated data) in order to detect a shift in the means. CLIMATOL can take advantage of metadata.

Inspired by Toreti *et al.* (2009), the Kolmogorov–Zurbenko adaptive filter (KZA; Zurbenko *et al.*, 1996) was applied to the precipitation only, as an absolute method (i.e., considers only the time sequence of a single station) to check the behaviour of the time series. The KZA filter was developed to detect breaks in non-parametric signals embedded in heavy background noise. It detects sudden changes over a low frequency signal of any nature submerged in heavy noise (Zurbenko and Sun, 2017). This analysis was conducted using the R package “kza” (Close and Zurbenko, 2016). However, whereas Toreti *et al.* (2009) used the KZA filter for one station at a time; in our study, it was done simultaneously for at least three stations from the same region. This approach was chosen to reduce false alarms by comparing the signals as well as the sample variance. An example of implementing the KZA filter is shown in Figure 2, and a scheme of the whole homogenization routine is presented in Figure 3.

For two extremely arid stations located in a region with sparse meteorological stations, which may impair the reliability of relative homogeneity tests, we have applied a few absolute homogeneity tests for Sedom and Elat (stations numbers 58 and 60, respectively): Pettit, 1979; SNHT (Alexandersson, 1986); KZA (Zurbenko *et al.*, 1996); Penalized Maximal F test (Wang, 2008) using RHtestV4 (Wang and Feng, 2013).

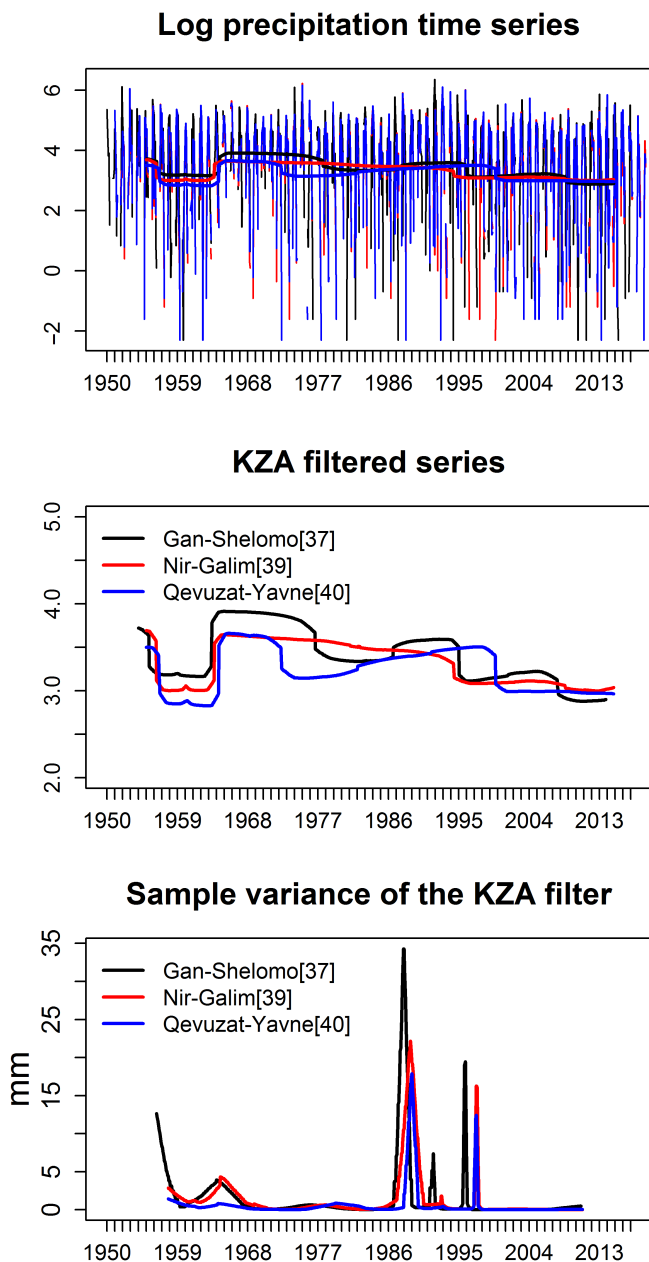


FIGURE 2 Upper panel: Monthly log precipitation time series of three stations (thin lines) and their filtered series (thick lines). Middle panel: KZA filter of three stations. Lower panel: Sample variance of the KZA filter [Colour figure can be viewed at wileyonlinelibrary.com]

After integrating these objective methods in addition to relevant metadata from the comprehensive IMS archive, the final decision on a BP location was made by affirming two major criteria: At least two methods detected a similar BP (± 1 year) or only one method detection plus metadata support. It should be noted that metadata was used only after the detection phase to validate the results (i.e., we did not force any BP merely because of metadata).

The temperature adjustment was made by applying the two factors ANOVA approach described by Caussinus and

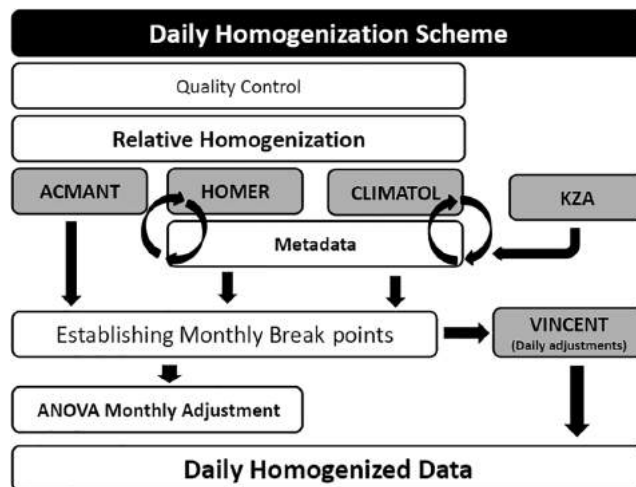


FIGURE 3 The homogenization scheme, applying relative methods: ACMANT, HOMER and CLIMATOL. For precipitation, an extra absolute test was added—KZA. After the breakpoint detection, the daily adjustments were derived from the monthly adjustments using the Vincent method

Mestre (2004) to the monthly data before the detected BP to correspond with the most recent homogenous period. The daily adjustments were derived from the monthly adjustments using the Vincent method (Vincent *et al.*, 2002). These adjustments were obtained by linear interpolation between the monthly correction factors. Although more sophisticated methods exist to adjust the higher order moment of the distribution, for example, HOM (Della-Marta and Wanner, 2006), HOMAD (Toreti *et al.*, 2010a), SPLIDHOM (Mestre *et al.*, 2011) and PM algorithm (Trewin, 2013), they depend on very high correlations between neighbouring time series (above 0.9), which must contain non-overlapping breaks. If these conditions are not met, it has been proven (Mestre *et al.*, 2011) that the most conservative option described in Vincent *et al.* (2002), provides better results. For the daily precipitation, we have applied the monthly correction factor (i.e., the ratio) for each day, following similar reasoning.

2.4 | The extreme indices

While monthly means provide useful climatological information to detect slow climate change processes, environmental impacts are often the result of short-term phenomena occurring well into the distribution tails of daily data (Zhang *et al.*, 2011). Thus, in order to gain a uniform perspective on observed changes in weather and climate extremes, a core set of 27 indices was defined by the Expert Team on Climate Change Detection and Indices (ETCCDI), which were actively coordinated by the CLIVAR/CCI/JCOMM. These indices are designed to monitor the changes in the frequency

TABLE 1 The extreme temperature and precipitation indices recommended by the expert teams (ET)

Index	Indicator name	Definitions	ET	Unit
<i>Temperature indices</i>				
1	FD0	Frost days	Annual count when TN (daily minimum) < 0°C	ETCCDI Days
2	ID0	Ice days	Annual count when TX (daily maximum) < 0°C	ETCCDI Days
3	SU25	Summer days	Annual count when TX (daily maximum) > 25°C	ETCCDI Days
4	TR20	Tropical nights	Annual count when TN (daily minimum) > 20°C	ETCCDI Days
5	FD2	Frost days 2	Annual count when TN < 2°C	ET-SCI Days
6	SU30	Hot days	Annual count when TX ≥ 30°C	ET-SCI Days
7	SU35	Very hot days	Annual count when TX ≥ 35°C	ET-SCI Days
8	DTR	Diurnal temperature range	Monthly mean difference between TX and TN	ETCCDI °C
9	TN _n	Min T_{\min}	Monthly minimum value of daily minimum temperature	ETCCDI °C
10	TN _x	Max T_{\min}	Monthly maximum value of daily minimum temperature	ETCCDI °C
11	TX _x	Max T_{\max}	Monthly maximum value of daily maximum temperature	ETCCDI °C
12	TX _n	Min T_{\max}	Monthly minimum value of daily maximum temperature	ETCCDI °C
13	TX10p	Cool days	Percentage of days when TX < 10th percentile	ETCCDI %
14	TX90p	Warm days	Percentage of days when TX > 90th percentile	ETCCDI %
15	TN10p	Cool nights	Percentage of days when TN < 10th percentile	ETCCDI %
16	TN90p	Warm nights	Percentage of days when TN > 90th percentile	ETCCDI %
17	WSDI	Warm spell duration indicator	Annual count of days with at least 6 consecutive days when TX > 90th percentile	ETCCDI Days
18	WSDI3	Warm spell duration indicator	Annual count of days with at least 3 consecutive days when TX > 90th percentile	ET-SCI Days
19	CSDI	Cold spell duration indicator	Annual count of days with at least 6 consecutive days when TN < 10th percentile	ETCCDI Days
20	CSDI3	Cold spell duration indicator	Annual count of days with at least 3 consecutive days when TN < 10th percentile	ET-SCI Days
21	TX3TN3 ^a	Hot days and nights	Annual count of 3 consecutive days where both TX > 95th percentile and TN > 95th percentile	ET-SCI Number of events
<i>Precipitation indices</i>				
22	PRCPTOT	Annual total wet-day precipitation	Annual total precipitation from days ≥ 1 mm	ETCCDI mm
23	R1mm ^a	Number of wet days	Annual count of days when precipitation ≥ 1 mm	ETCCDI Days
24	R10mm	Number of heavy precipitation days	Annual count of days when precipitation ≥ 10 mm	ETCCDI Days
25	R20mm	Number of very heavy precipitation days	Annual count of days when precipitation ≥ 20 mm	ETCCDI Days
26	R50mm ^a	Number of days above 50 mm	Annual count of days when precipitation ≥ 50 mm	ETCCDI Days
27	R95p	Very wet days	Annual total precipitation when RR > 95th percentile	ETCCDI Mm
28	R99p	Extremely wet days	Annual total precipitation when RR > 99th percentile	ETCCDI Mm
29	R95pTOT	Contribution from very wet days	100*R95p/PRCPTOT	ET-SCI %
30	R99pTOT	Contribution from extremely wet days	100*R99p/PRCPTOT	ET-SCI %
31	RX1day	Max 1-day precipitation amount	Monthly maximum 1-day precipitation	ETCCDI mm
32	RX5day	Max 5-day precipitation amount	Monthly maximum consecutive 5-day precipitation	ETCCDI mm

(Continues)

TABLE 1 (Continued)

Index	Indicator name	Definitions	ET	Unit
33 SDII	Simple daily intensity index	Annual total precipitation divided by the number of wet days (defined as precipitation ≥ 1 mm) in the year	ETCCDI	mm/day
34 CWD	Consecutive wet days	Maximum number of consecutive days when precipitation ≥ 1 mm	ETCCDI	Days
35 CDD	Consecutive dry days	Maximum number of consecutive days when precipitation < 1 mm	ETCCDI	Days
36 CDD-DJF ^b	Consecutive dry days	Maximum number of consecutive days when precipitation < 1 mm, between December to February		Days
37 CDD-NDJFM ^b	Consecutive dry days	Maximum number of consecutive days when precipitation < 1 mm between November to March		Days
38 CDD-NDJFMA ^b	Consecutive dry days	Maximum number of consecutive days when precipitation < 1 mm between November to April		Days

^aUser-defined index threshold.

^bThe authors' modification of CDD index.

and/or intensity of “moderately” extreme events, by focusing on events that typically occur several times per year rather than high-impact once-in-a-decade weather events (Klein Tank *et al.*, 2009; Zhang *et al.*, 2011). Additionally, the WMO Commission for Climatology (CCI) established an Expert Team on Sector-specific Climate Indices (ET-SCI). The ET-SCI has developed a number of climate indices that consider health, water and agriculture sectors requirements alongside the ETCCDI indices (Alexander and Herold, 2015). In order to calculate these extreme indices derived from daily data, “R” software packages were developed RclimDex for the ETCCDI indices (Zhang and Yang, 2004) and ClimPACTv2 for the ET-SCI indices (Alexander and Herold, 2015).

These climate extreme indices are calculated based on daily observational minimum and maximum temperatures and daily precipitation records. In this study, most indices were calculated using ClimPACTv2, which includes Zhang's *et al.* (2005b) bootstrapping procedure to determine climatological percentile thresholds in order to avoid discontinuities in the indices time series at the beginning or end of the base period. The selected base period for the percentile indices was 1961–1990.

In order not to artificially truncate the rainy season in December (in Israel it is between October and May), the rainy season is defined as starting on August 1 and ending on July 31 of the next year. Therefore, the study period includes 67 rainy seasons 1950/1–2016/7 for the precipitation indices. Additional index calculations such as consecutive dry days (CDD) were performed for only the wet

months (e.g., CDD-DJF, CDD-NDJFM). A list of the 38 selected indices with their acronyms and short explanations is presented in Table 1.

2.5 | Regional average series

To summarize the changes observed over Israel, regional averages for every index were computed. The regional averaged temperature indices were computed as an unweighted mean of the indices at individual stations relative to their climatological averages for period 1961–1990. This calculation involved the 24 long-term temperature stations only.

The regional average indices for precipitation were based on weighting the anomalies values (reference period 1961–1990) across the region, where the weights were determined by Thiessen polygons for every station as suggested by Jones and Hulme (1996). This calculation considered 58 stations out of 60 since we did not include the two most arid stations (Sedom[58] and Elat[60]).

2.6 | Trend calculation

The time series of the trends of the various indices were calculated for two different periods, 1950–2017 and 1988–2017. The analysis was done using the robust non-parametric Mann–Kendall test (Mann, 1945; Kendall, 1955) with Sen's slope estimator (Sen, 1968), since it is not affected by the distribution of the data, or is it sensitive to outliers. All the time series were pre-whitened in order to correct the Mann–Kendall test for serial autocorrelation

(Zhang *et al.*, 2000; Wang and Swail, 2001). We consider a trend to be significant if it is statistically significant at the 5% level. This trend analysis was conducted using the R package “zyp” (Bronaugh and Werner, 2013).

Linear trends are not necessarily the best fit for the observed changes. In order to better represent the decadal variations, a LOWESS smoother (Cleveland, 1979) was added to our regional anomalies time series plots.

3 | RESULTS

The thorough homogenization procedure depicted in Section 2.3 reveals that the vast majority of the temperature time series are tainted by non-climatic factors. It was found that on average each station has approximately 3.5 BPs (every ~16 years). More than 60% from the detected BPs have metadata (documentary information on known changes) support. Figure 4 shows an example of the dissimilarity between raw versus homogenized records for the TN in En-Hahores (station number 16, Table S1). This time series has four BPs (the first three breaks caused due to relocation and the fourth due to sensor replacement). Hence, the trend was changed dramatically from non-significant $0.1^{\circ}\text{C}/\text{decade}$ [$-0.17, 0.37$] to highly significant warming $0.26^{\circ}\text{C}/\text{decade}$ (raw vs. adjusted records, respectively), stressing the importance of homogenization to eliminate or at least minimize these artificial non-climate factors in order to attain a reliable climatic trend. Our previous study discussed these issues in greater detail, exploring a few stations across Israel (Yosef *et al.*, 2018). Of the 60 precipitation stations involved, only 15 BPs were detected over 12 stations.

Table 2 summarizes the regional trends with 95% confidence intervals for each index over the long-term period 1950–2017 and for the last 30 years since 1988. For several selected indices, the annual or seasonal regional time series

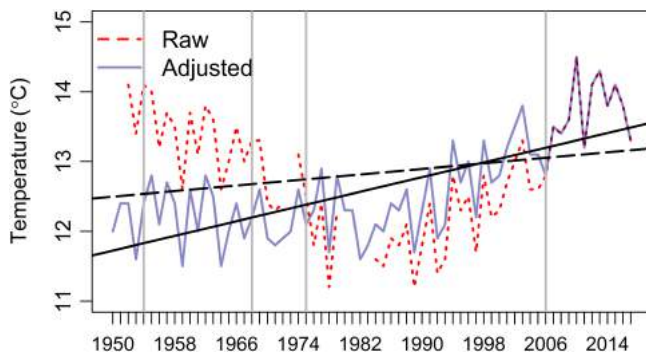


FIGURE 4 Homogenized (solid blue line) versus raw (dashed red line) and their corresponding trend lines (solid vs. dashed, respectively) for the TN records in En-Hahores. Breakpoint locations are denoted by grey vertical lines [Colour figure can be viewed at wileyonlinelibrary.com]

graphs are shown when the spatial annual trends are presented on maps.

3.1 | Trends in temperature indices

3.1.1 | Mean temperature

Regional trends of the annual maximum, minimum and mean daily temperature are shown in Table 2. Statistically significant warming is evident over a long period more intensely for the last 30 years. A highly significant positive long-term trend was found for the mean minimum temperature (TNm) with $0.24^{\circ}\text{C}/\text{decade}$, whereas the mean maximum temperature (TXm) trend was $0.19^{\circ}\text{C}/\text{decade}$. This higher trend is for the TNm, as opposed to the TXm manifested in a significant negative diurnal temperature range (DTR). The short-term changes of the maximum, minimum and mean temperature are similar, characterized by highly significant increasing trends of about $\sim 0.55^{\circ}\text{C}/\text{decade}$, whereas a weak positive (non-significant) DTR trend was found.

Figures 5 and 6 present the regional averaged anomalies time series of seasonal TXm and TNm, respectively. Significant warming trends were found for both variables in all seasons with stronger trends for 1988–2017. One exception to this was recorded in the winter, with non-significant trends in both parameters for the long period only (i.e., significant warming trends were found in the recent period). Warming trends for both variables were strongest during the summer and spring seasons, followed by the autumn season.

3.1.2 | Absolute annual maximum and minimum temperature indices

The annual regional change of the absolute warmest day/night (TXx, TNx) and coldest day/night (TXn, TNn) temperatures of the year is presented in Table 2, where the areal averages of the anomalies are shown in Figure 7. The long-term changes are positive, while only the TNx shows a significant increase of 0.26 and $0.62^{\circ}\text{C}/\text{decade}$ for the long and short periods, respectively. The significant tendency towards higher temperature in the warmest night index (TNx) is mainly manifested in the coastal plain, lowlands and the northeastern parts of the country for the last 30 years (bottom panel of Figure 8). While the TXx and TXn show non-significant warming tendencies, the TNn shows a general mild non-significant decrease in most of the stations located in the northern part of the country over the shorter period.

3.1.3 | Above or below specific temperature threshold

Since Israel is located in a subtropical region characterized by Mediterranean to arid climate, indices that count the

TABLE 2 The regional temperature and precipitation trends per decade for 1950–2017 and 1988–2017^a

Index	1950–2017	1988–2017	Unit
FD0	0 (−0.06, 0.06)	0 (−0.14, 0.28)	Day
ID0	-	-	Day
SU25	1.88 (0.29, 3.49)	8.58 (4.81, 12.77)	Day
TR20	6.88 (4.3, 9.17)	13.58 (8.99, 16.05)	Day
FD2	−0.06 (−0.33, 0.17)	0.25 (−0.9, 0.88)	Day
SU30	4.41 (1.85, 7.05)	9.64 (6.11, 13.69)	Day
SU35	1.71 (0.55, 3.15)	4.5 (1.73, 6.93)	Day
TNm ^b	0.24 (0.15, 0.33)	0.55 (0.38, 0.71)	°C
TXm ^b	0.19 (0.07, 0.31)	0.56 (0.39, 0.75)	°C
TMm ^b	0.21 (0.12, 0.32)	0.53 (0.4, 0.71)	°C
DTR	− 0.07 (−0.11, −0.03)	0.05 (−0.08, 0.17)	°C
TNn	0.06 (−0.09, 0.2)	0 (−0.5, 0.54)	°C
TNx	0.26 (0.12, 0.41)	0.62 (0.31, 1)	°C
TXx	0.12 (−0.07, 0.28)	0.19 (−0.49, 0.85)	°C
TXn	0.09 (−0.1, 0.26)	0.19 (−0.58, 1)	°C
TX10p	− 1.14 (−1.8, −0.45)	− 2.36 (−4.06, −0.91)	%
TX90p	1.45 (0.43, 2.35)	5.11 (3.51, 6.36)	%
TN10p	− 1.26 (−1.81, −0.77)	− 1.77 (−3.26, −0.78)	%
TN90p	2.57 (1.52, 3.65)	6.9 (5.19, 8.08)	%
WSDI	1.2 (0.09, 2.45)	8.03 (4.53, 12.12)	Day
WSDI3	4.17 (1.12, 6.92)	14.92 (10.89, 18.89)	Day
CSDI	−0.08 (−0.33, 0.08)	−0.27 (−0.83, 0.44)	Day
CSDI3	− 1.25 (−2.05, −0.54)	−2.04 (−4.26, −0.01)	Day
TX3TN3	0.03 (0, 0.06)	0.2 (0.05, 0.35)	Number of events
PRCPTOT	−4.4 (−17.67, 10.58)	−25.42 (−73.4, 14.25)	mm
R1mm	−0.52 (−1.53, 0.65)	−3 (−6.25, 0.11)	Day
R10mm	−0.2 (−0.64, 0.26)	−1 (−2.67, 0.47)	Day
R20mm	−0.04 (−0.31, 0.22)	−0.44 (−1.13, 0.31)	Day
R50mm	0 (−0.04, 0.06)	0 (−0.17, 0.17)	Day
R95p	1.15 (−5.74, 7.04)	−1 (−21.8, 17.88)	mm
R99p	1.84 (−0.95, 4.33)	3.73 (−6, 13.75)	mm
R95pTOT	0.33 (−0.67, 1.39)	−0.06 (−4.86, 5.23)	%
R99pTOT	0.44 (−0.12, 1)	0.65 (−1.76, 2.93)	%
RX1day	0.5 (−0.68, 1.71)	0.25 (−3.64, 4.94)	Mm
RX5day	−0.44 (−3.37, 3.03)	1 (−12.16, 19.2)	Mm
SDII	0.06 (−0.14, 0.24)	0.09 (−0.72, 1.13)	Mm/day
CWD	−0.07 (−0.21, 0.05)	0 (−0.47, 0.46)	Day
CDD-annual	−0.16 (−2.5, 2.32)	−2.5 (−8.84, 6.38)	Day
CDD-DJF	−0.03 (−0.72, 0.66)	0.57 (−2.11, 3.65)	Day
CDD-NDJFM	0.28 (−0.44, 1.07)	1.78 (−0.8, 4.7)	Day
CDD-NDJFMA	0.81 (−0.24, 1.8)	1.99 (−2.69, 4.92)	Day

^aThe 95% confidence intervals are shown in parentheses. Values for trends significant at the 5% level are set bold face.^bThe average maximum, minimum and the mean temperature (TXm, TNm, and TMm, respectively).

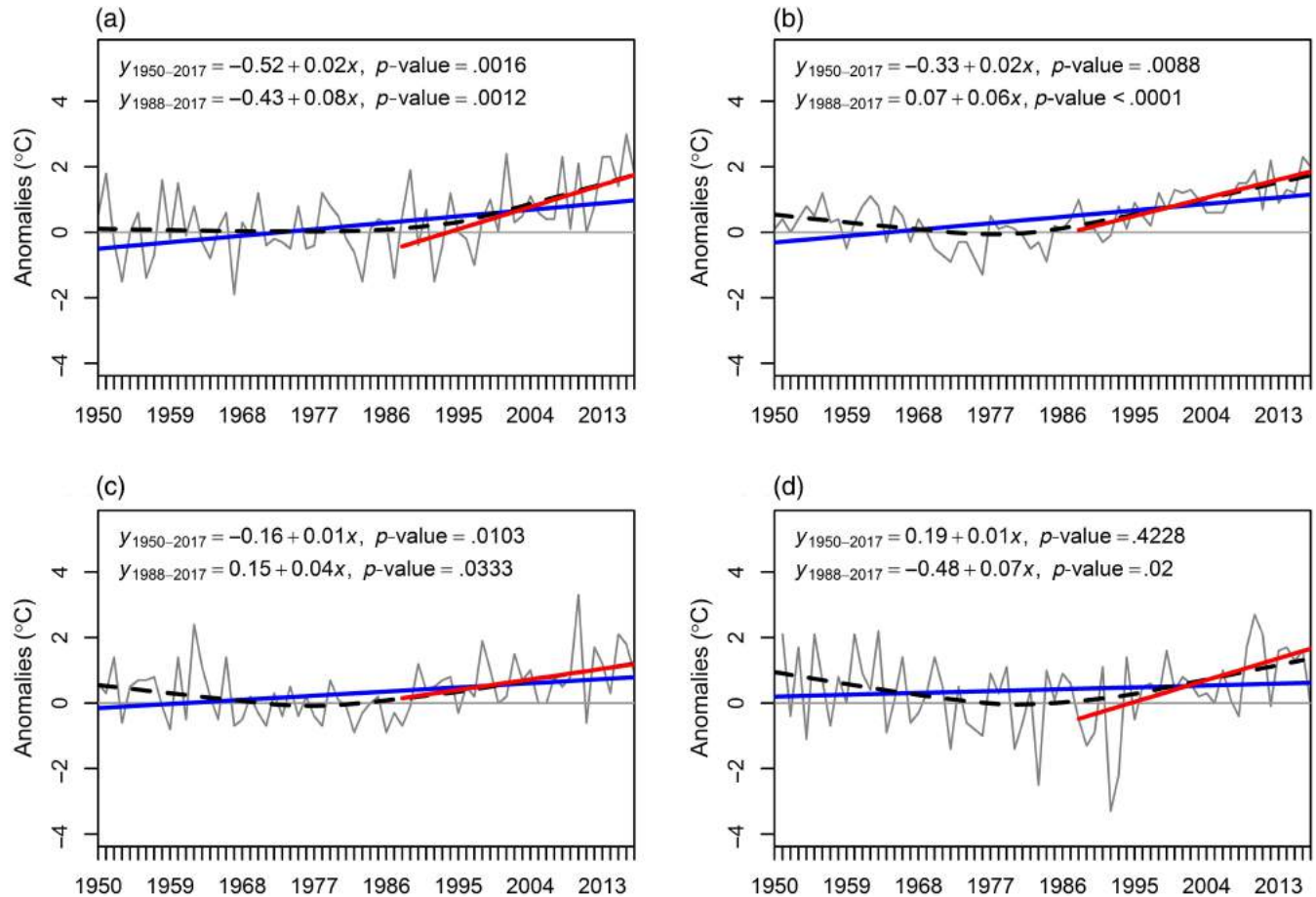


FIGURE 5 Regional averaged anomaly series (relative to 1961–1990) of seasonal TX. Blue lines represent linear trends for 1950–2017. Red lines represent linear trends for 1988–2017. Dashed black lines are based on the LOWESS smoother. (a) Spring (March, April, May). (b) Summer (June, July, August). (c) Autumn (September, October, November). (d) Winter (December, January, February) [Colour figure can be viewed at wileyonlinelibrary.com]

number of frost/icing days (FD0, ID0) are quite rare, whereas the index of summer days (SU25) is too frequent. Thus, few ET-SCI indices that are more typical to the south-eastern corner of the Mediterranean Sea were calculated: FD2 is the number of frost days, SU30 is the number of hot and SU35 is the number of very hot days.

The regional average of the number of hot days, very hot days and tropical nights (TR20) has significantly increased during the period 1950–2017 with stronger increases (more than double) during 1988–2017. The FD2 index shows non-significant weak negative (positive) trends for the long (short) period (Table 2).

3.1.4 | Percentile-based temperature indices

Indices that count the occurrences of temperatures below the 10th percentile (cool days/nights) and above the 90th percentile (warm days/nights) represent the upper and lower tails of the distribution functions of daytime and nighttime temperatures that have experienced significant shifts in most regions of the globe (Donat and Alexander, 2012).

The regional long trends of TX10p and TN10p indices have decreased by -1.14 and -1.26% /decade with an extra slight reduction to -2.36 and -1.77% /decade in the last 30 years, respectively (both statistically significant). Conversely, regional long-term trends of TX90p and TN90p indices have significantly increased by 1.45 and 2.57% /decade with additional increases to 5.11 and 6.9% /decade during the period 1988–2017 (Table 2), respectively.

Figure 9 shows the spatial distribution of trends for both the periods, 1950–2017 and 1988–2017, in the annual TX10p, TX90p, TN10p and TN90p. The spatial TX10p and TN10p indices show mainly statistically significant decreasing trends in the number of cool days and nights with similar magnitudes for both periods at most of the stations. Nevertheless, the downward trends in the northern parts of the country are more pronounced over the 1988–2017 period when compared to the 1950–2017 period for TX10p, denoting that roughly the coldest part of the country has fewer “cool day” events. Furthermore, TN10p shows a non-significant decreasing trend for all of the Eastern valleys stations (located at -135 to -388 m below sea level), implying

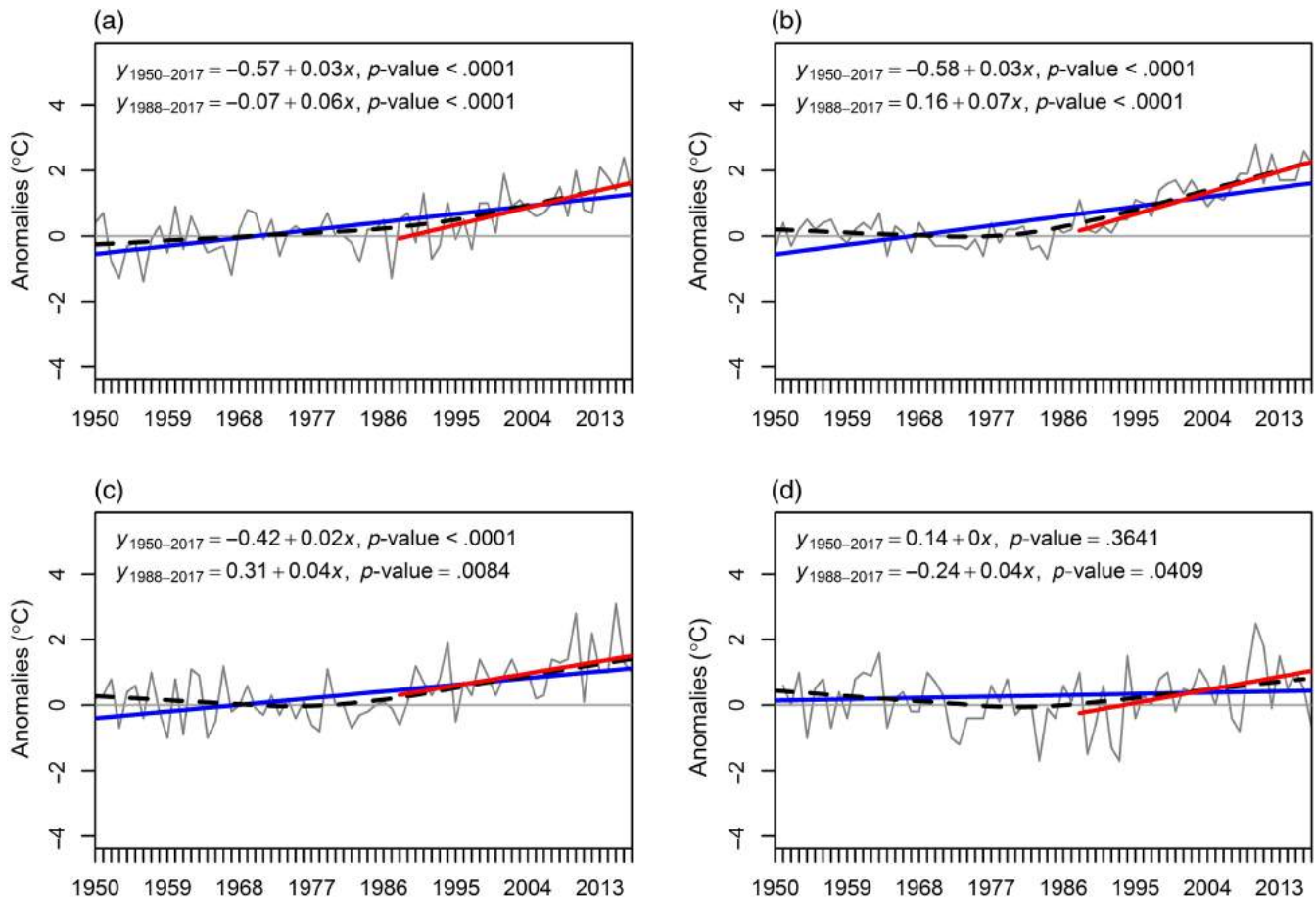


FIGURE 6 Same as Figure 5 but for TN. (a) Spring (March, April, May). (b) Summer (June, July, August). (c) Autumn (September, October, November). (d) Winter (December, January, February) [Colour figure can be viewed at wileyonlinelibrary.com]

that there is no statistically significant change in the number of cool nights in the hottest part of the country.

The spatial annual percentage of warm days (TX90p) and nights (TN90p) indices have a strong pattern of increasing trends at most of the stations. While the long-term trend of TX90p shows coherent strong spatial patterns ($\sim 1\%$ /decade), the TN90p shows pronounced trends mainly across the coastal plain ($\sim 3\%$ /decade), whereas in the other parts of the country the trends are about $\sim 1\%$ /decade. For the short period, a stronger significant upward trend was found for TX90p (mainly across the coastal plain) and TN90p for the entire country except for the mountainous stations (above ~ 450 m) that showed weaker upward statistically significant trends in the latter index.

Figure 10 shows an example of the seasonal TN90p regional averaged anomaly series. The figure illustrates that the general increase in the number of warm nights mainly occurred in the 1990s for all seasons. While the summer has the highest absolute trends (14.5% /decade) for 1988–2017 (which are three times higher) compared to the long period, the winter has undergone the most pronounced change, from a non-significant increasing long-term trend (0.6% /decade) to a statistically significant trend of 4.6% /decade. The spring

and autumn have doubled their trend magnitude to 2.8 and 4.3% /decade over the last 30 years, respectively. The seasonal TX90p anomaly series is similar to TN90p but with weaker and less statistically significant trends (not shown).

The seasonal trends in TX10p are typically weaker than those in TN10p (not shown). Statistically significant decreasing trends have been observed for all the seasons except for the winter for both indices and periods. Figure 11 displays the averaged regional anomalies of TX10p for each season. Interestingly, it is noticeable that the interannual variability becomes smaller around the end of the 1990s in all seasons, especially for the summer (JJA). Generally, this seasonal behaviour of TX10p is similar to TN10p, indicating that the percentage of days when the temperature is less than the 10th percentile were rarely measured mainly in the summer since the end of the 1990s.

3.1.5 | Warm spells and cold spells

Figure 12 presents the spatial trends of warm spell duration index (WSDI) and CSDI3 over 1950–2017 and 1988–2017. The duration of WSDI (CSDI3) has a slight increase

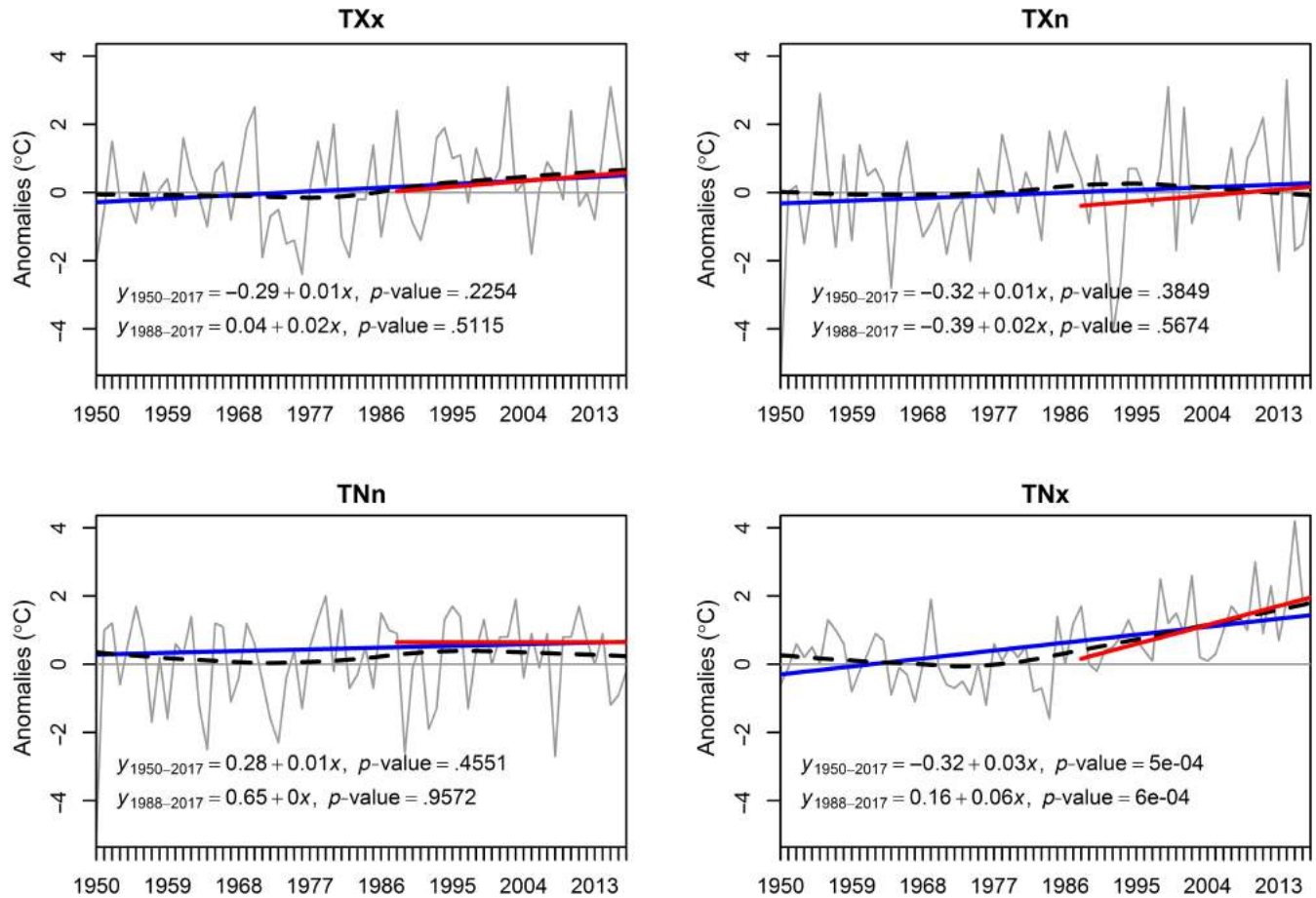


FIGURE 7 Same as Figure 5 except for regional averaged anomaly series (relative to 1961–1990) of TXx, TXn, TNn, TNx (unit: °C/decade) [Colour figure can be viewed at wileyonlinelibrary.com]

(decrease) in some stations, which is statistically significant during the period 1950–2017. The trends in WSDI have been much stronger in the last 30 years throughout the entire country. Figure 13 shows the regional averaged anomaly series of WSDI. A much stronger positive trend for the shorter period was found (1.2 vs. 8 days/decade). However, most of this increase has occurred since about 1990. While the WSDI shows significant increase for the last 30 years, a weak regional decrease that was found for the CSDI3 was not statistically significant over 1988–2017 (Table 2).

3.2 | Trends in precipitation

We have observed a general decrease in the total amount of precipitation and in the number of wet days above different thresholds (1, 10, and 20 mm per day) although statistically non-significant on a regional scale (Table 2) for both periods, 1950–2017 and 1988–2017.

Figure 14 shows the trend in the annual total precipitation (PRCPTOT) and in the contribution from the very wet days index (R95pTOT) for both periods together with their regional averaged anomalies. Although precipitation is

characterized by much stronger temporal and spatial variability than what was seen in the temperature, we have found a coherent spatial pattern change for most of the indices. Thus, a general decrease is most pronounced when trends are calculated over the shorter period unlike R95pTOT index, which has been increasing mainly in the northern part of the country over the last 30 years. These indicate a tendency towards more intense rainy days, but once again the trends were not statistically significant. It should be noted that 1992 was an outstanding, breaking record winter in terms of the total precipitation amount in most of the stations. Therefore, when analysing trend for the last three decades, in which 1992 is at the beginning of the time series, a much stronger downward trend is obtained.

Figure 15 presents the trend in the annual number of wet days when precipitation was ≥ 1 mm and ≥ 10 mm per day. A decrease in the number of wet days (R1mm) and heavy precipitation days (R10mm) was found. The centre of the country was found to be the only area (out of all the precipitation indices) exhibiting a statistically significant decreasing trend (more than 4 days/decade) for the R1mm over the period 1988–2017.

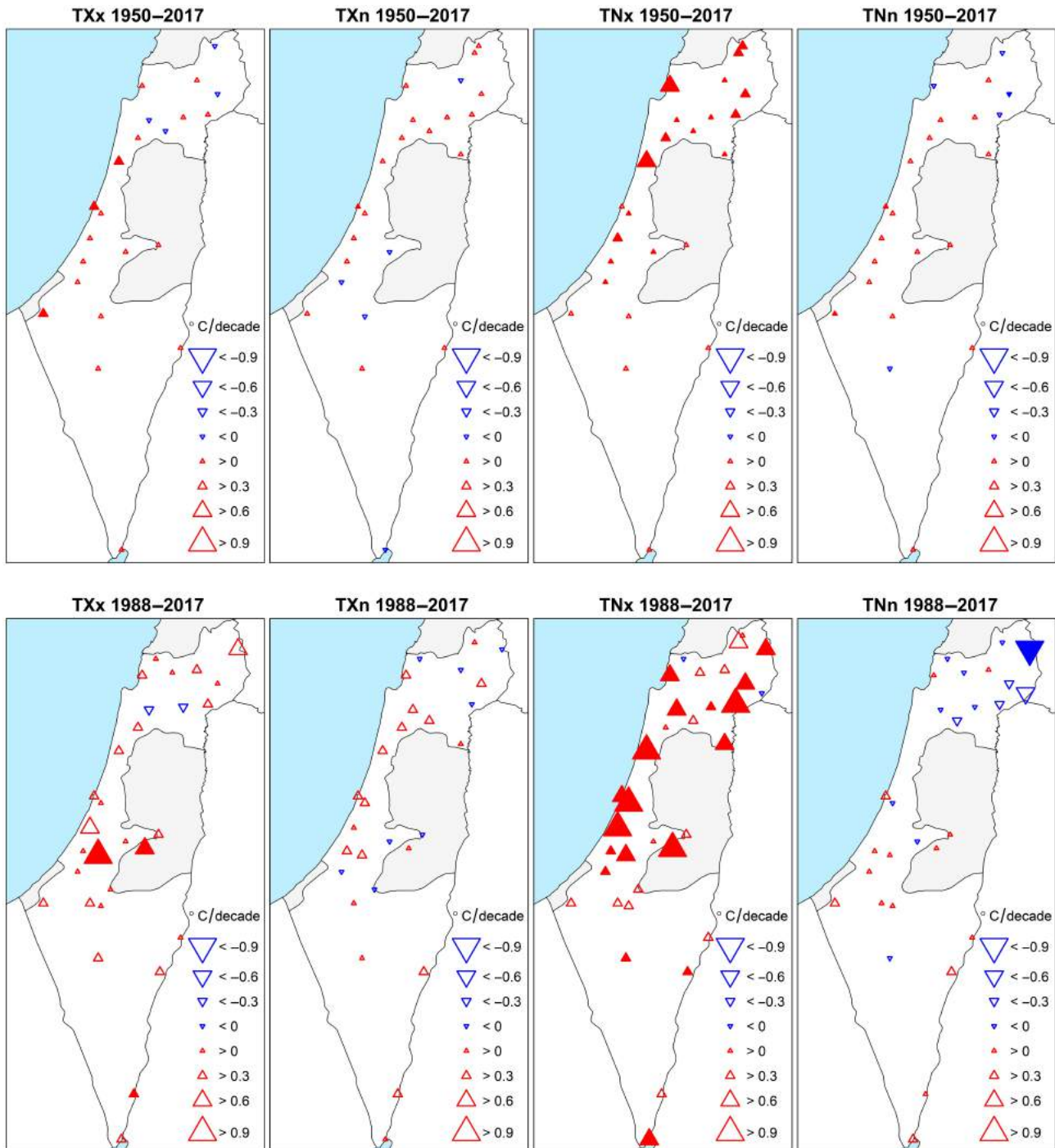


FIGURE 8 Trend in the annual maximum (TXx, TNx) and minimum (TXn, TNn) values of daily temperature for the period 1950–2017 (upper panels) and 1988–2017 (lower panels). Upward red triangles represent increasing trends, and downward blue triangles represent decreasing trends. Different sizes of triangles indicate different magnitudes of trends. Significant changes ($p \leq .05$) are indicated by filled triangles (unit: °C/decade) [Colour figure can be viewed at wileyonlinelibrary.com]

While the maximum 1 day precipitation amount (RX1day) index shows weak increasing trends, RX5days index (highest amount for 5 days) shows a general light decreasing trend (Table 2) for the long period. However, these indices show a general increasing trend in the northern part of the country, central mountains, southern lowlands

and coastal plain during the last 30 years (not shown). Both long and short trends are statistically not significant (characterized by wide confidence intervals).

The CDD index is the length of the longest dry spell in a predefined period (e.g., annually, December–February, etc.). Figure 16 presents the spatial distribution of trends for

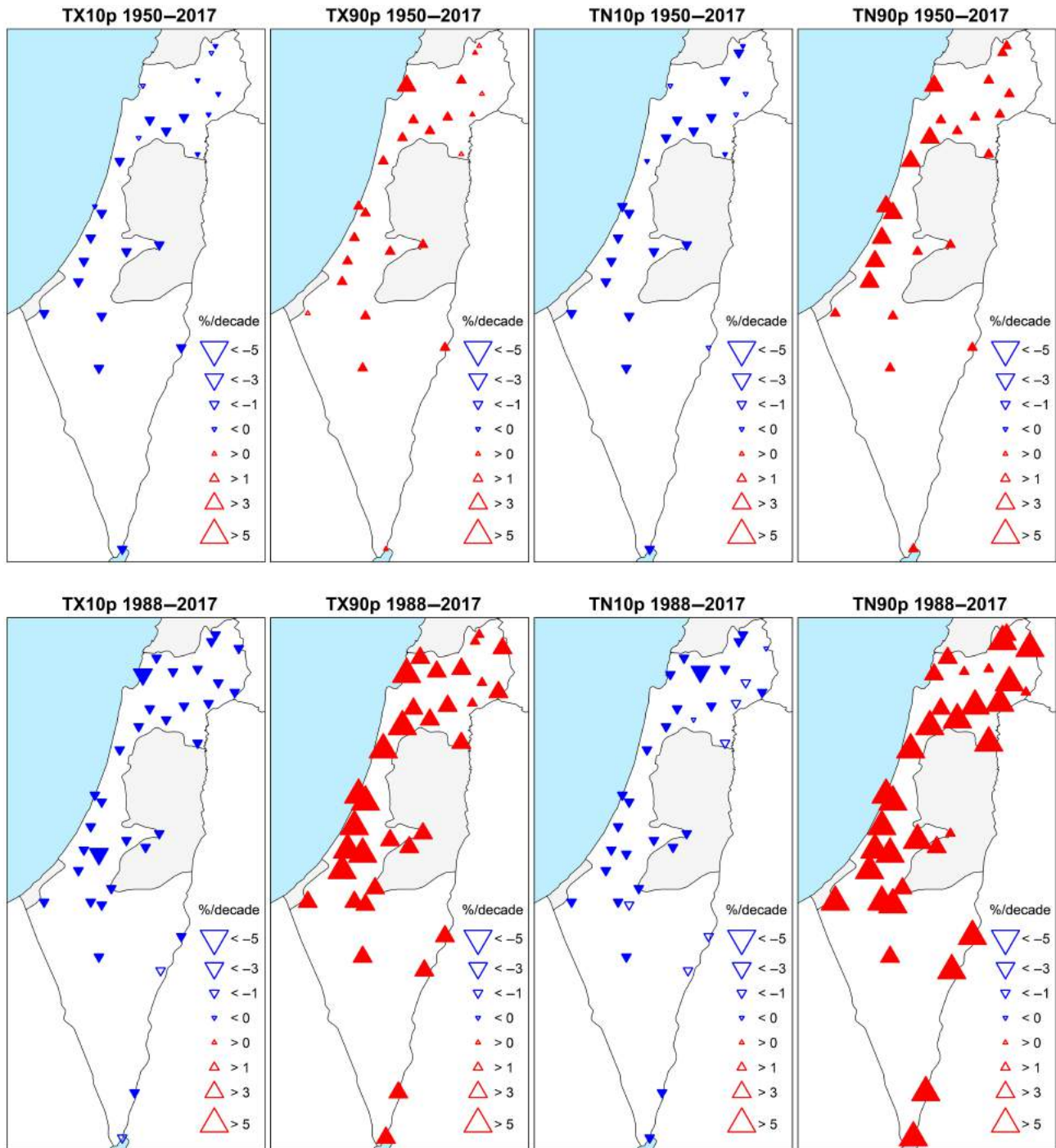


FIGURE 9 Same as Figure 8 except for the annual TX10p (cool days), TX90p (warm days), TN10p (cool nights) and TN90p (warm nights) (unit: %/decade) [Colour figure can be viewed at wileyonlinelibrary.com]

different periods of CDD. The duration of annual CDD, that is, the number of dry days between adjacent years, shows mainly non-significant trends towards shorter duration of dry spells with stronger trends in the recent epoch. The long-term change in the CDD for the core winter months (DJF) shows a non-significant weak decrease as well, except for the northern tip of the country, characterized by a longer duration of CDD-DJF. For 1988–2017, most of the country

shows non-significant trends towards a longer duration of dry spells. The CDD for the whole wet season, whether it ended in March or in April, shows a general tendency towards non-significant increasing trends over 1950–2017. While for the short period, the CDD-NDJFM shows a general coherent strong non-significant increase, the CDD-NDJFMA shows a decrease in the northern part and an increase for most other areas (not significant). This may be

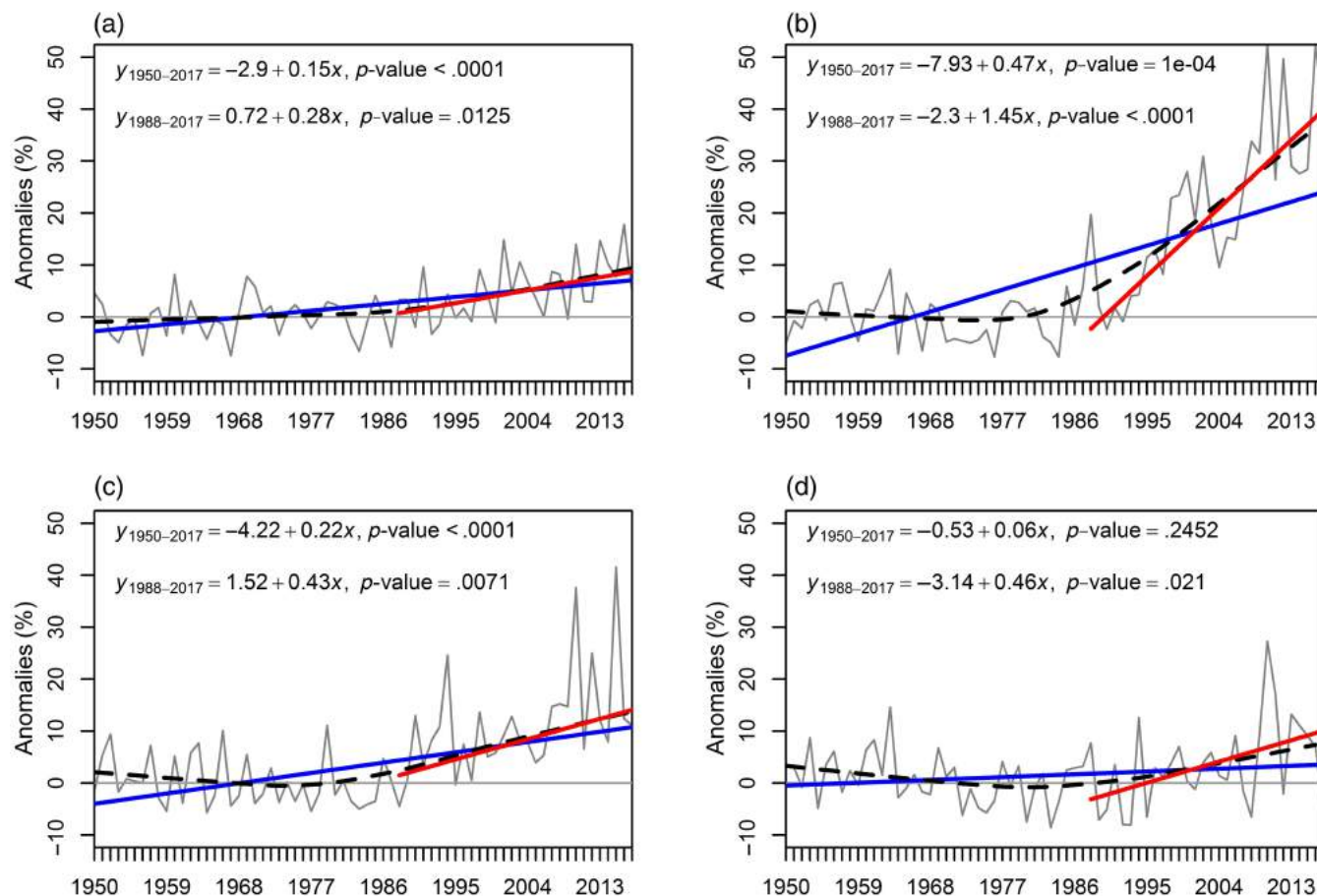


FIGURE 10 Same as Figure 5 except for the seasonal TN90p (warm nights) (unit: %/decade). (a) Spring (MAM). (b) Summer (JJA). (c) Autumn (SON). (d) Winter (DJF) [Colour figure can be viewed at wileyonlinelibrary.com]

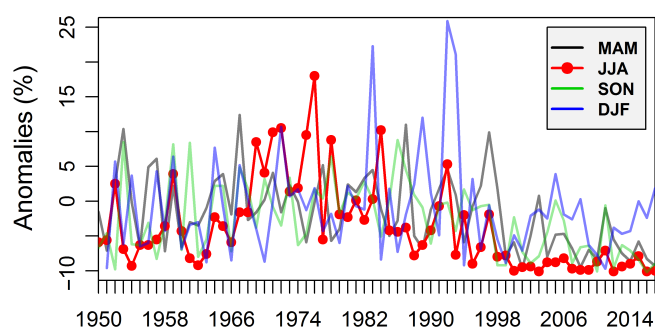


FIGURE 11 Averaged regional anomalies of TX10p for the spring (MAM), summer (JJA), autumn (SON) and winter (DJF) [Colour figure can be viewed at wileyonlinelibrary.com]

attributed to more rainy days during April in the northern area than in other parts of the country.

4 | DISCUSSION

A thorough homogenization procedure was carried out in order to reduce the biases of non-climatic factors and thus to

obtain more reliable trends. Results from the mean and extreme temperature analysis reveal significant warming trends. The warming observed in Israel is associated with more warm temperature events along with fewer cold events over the last 70 years. The higher warming trends of the TN (nighttime), as opposed to the TX (daytime), lead to a significant decrease in the DTR ($-0.07^{\circ}\text{C}/\text{decade}$) over the long-term period. This is consistent with other global and regional studies (Easterling *et al.*, 1997; Brunetti *et al.*, 2006; Klein Tank *et al.*, 2006; AlSarmi and Washington, 2011; Vincent *et al.*, 2012; Donat *et al.*, 2013; Barry *et al.*, 2018; Yosef *et al.*, 2018).

While most DTR decreases occurred prior to the 1980s, the recent period (1988–2017) is characterized by an increasing DTR trend with a similar magnitude for the TX and the TN simultaneously ($\sim 0.55^{\circ}\text{C}/\text{decade}$). As a consequence, the DTR exhibits non-significant trends ($0.05^{\circ}\text{C}/\text{decade}$ [$-0.08, 0.17$]), which are consistent with other recent studies (Thorne *et al.*, 2016; Barry *et al.*, 2018).

It should be noted that long-term increasing trends detected for both temperature parameters are not monotonic over the annual and seasonal time series (Figures 5–6). The

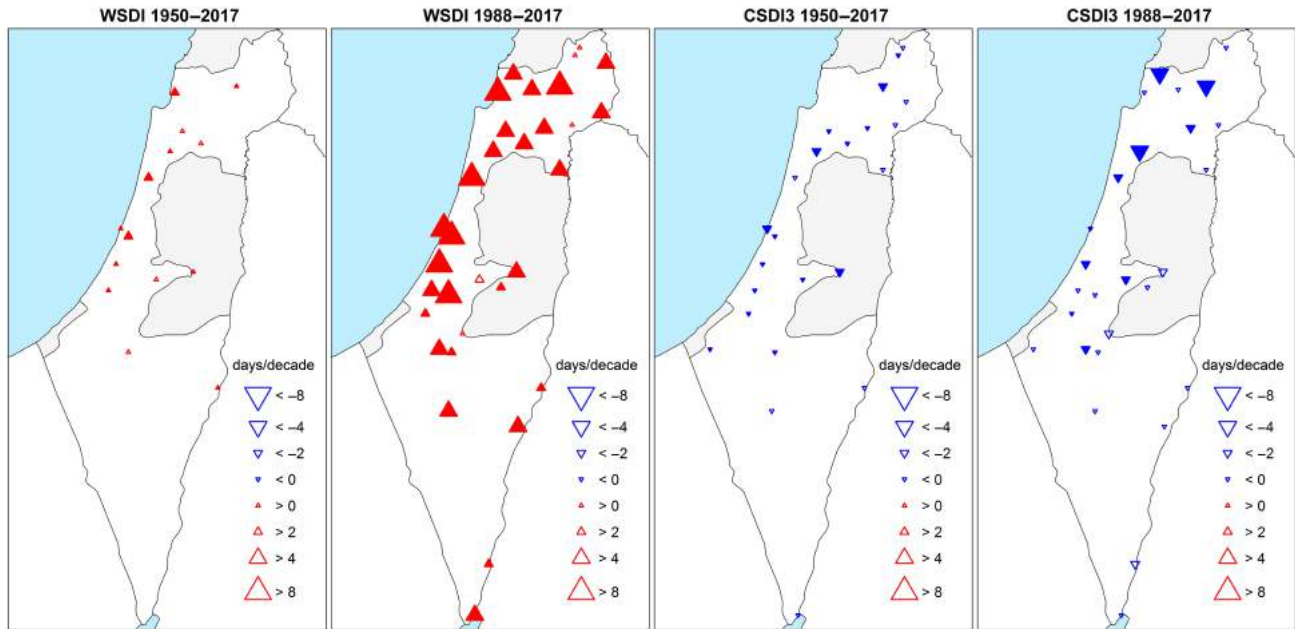


FIGURE 12 Same as Figure 8 except for the annual WSDI and CSDI3 (unit: days/decade) [Colour figure can be viewed at wileyonlinelibrary.com]

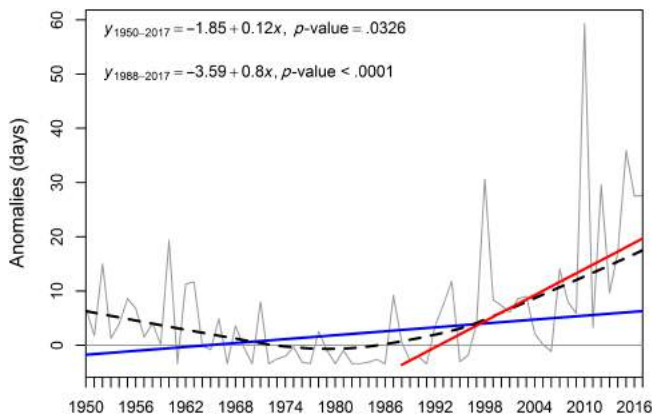


FIGURE 13 Same as in Figure 5 except for WSDI. (unit: days/decade) [Colour figure can be viewed at wileyonlinelibrary.com]

period from the 1950s until the end of the 1970s is typically characterized by a decreasing trend, or it oscillates around the mean value, in contrast to sharp increasing trends that occurred since the early 1990s in agreement with Yosef *et al.* (2018) for Israel and Tanarhte *et al.* (2012) for Greece, Turkey and the Levant region.

Annual and seasonal non-monotonic trends were also detected in the percentile-based indices of warm days (TX90p) and nights (TN90p), showing stronger trends (mainly across the coastal plain) in the last 30 years. The summer significantly leads these trends for both indices (and also the autumn). This summer phenomenon is consistent with other EM and Israel studies (Price *et al.*, 1999; Saaroni *et al.*, 2003; Domroes and El-Tantawi, 2005; Kostopoulou

and Jones, 2005; Ziv *et al.*, 2005; Shohami *et al.*, 2011; Tanarhte *et al.*, 2012; Mamara *et al.*, 2016; Yosef *et al.*, 2018). A continuous steady rise in temperatures at the 850 hPa for the summer over the Mediterranean and the EM (Saaroni *et al.*, 2003; Ziv *et al.*, 2005; Shohami *et al.*, 2011) together with a rapid increase in the occurrence of the weak Persian Trough (Saaroni *et al.*, 2010) may be related to this significant increase. Additionally, a weak Persian Trough is characterized by weak Etesian winds implying a reduction in the prevailing cool advection from the northwest (Saaroni *et al.*, 2003). This causes the marine inversion to descend and, as a consequence, the temperature rises, mainly in the mountains around noon. Relative humidity increases on the coastal plain and lowlands, leading to intense heat stress and warmer nights as reported in the results section of this paper. In addition, it was found (Shohami *et al.*, 2011) that the EM sea surface temperatures exhibited highly significant positive trends of 0.2–0.3°C/decade during the summer and the autumn of 1964–2003. All the above can be attributed to the sharp increases in the warm spells (WSDI, WSDI3) particularly in the coastal plain.

Since 1996, the winter exhibits consecutive warm years, where only 5 years were below average, introducing tremendously significant warmer winters (Figure 5d, Figure 6d, Figure 10d). In addition, a minor downward tendency that was not statistically significant was found for the cool days (TX10p) and nights (TN10p) during winter for both periods (not shown). Moreover, a general decrease in the cold spells' duration (CSDI, CSDI3) was found where only the regional long-term trend of the CSDI3 index was statistically significant (Table 2). This can

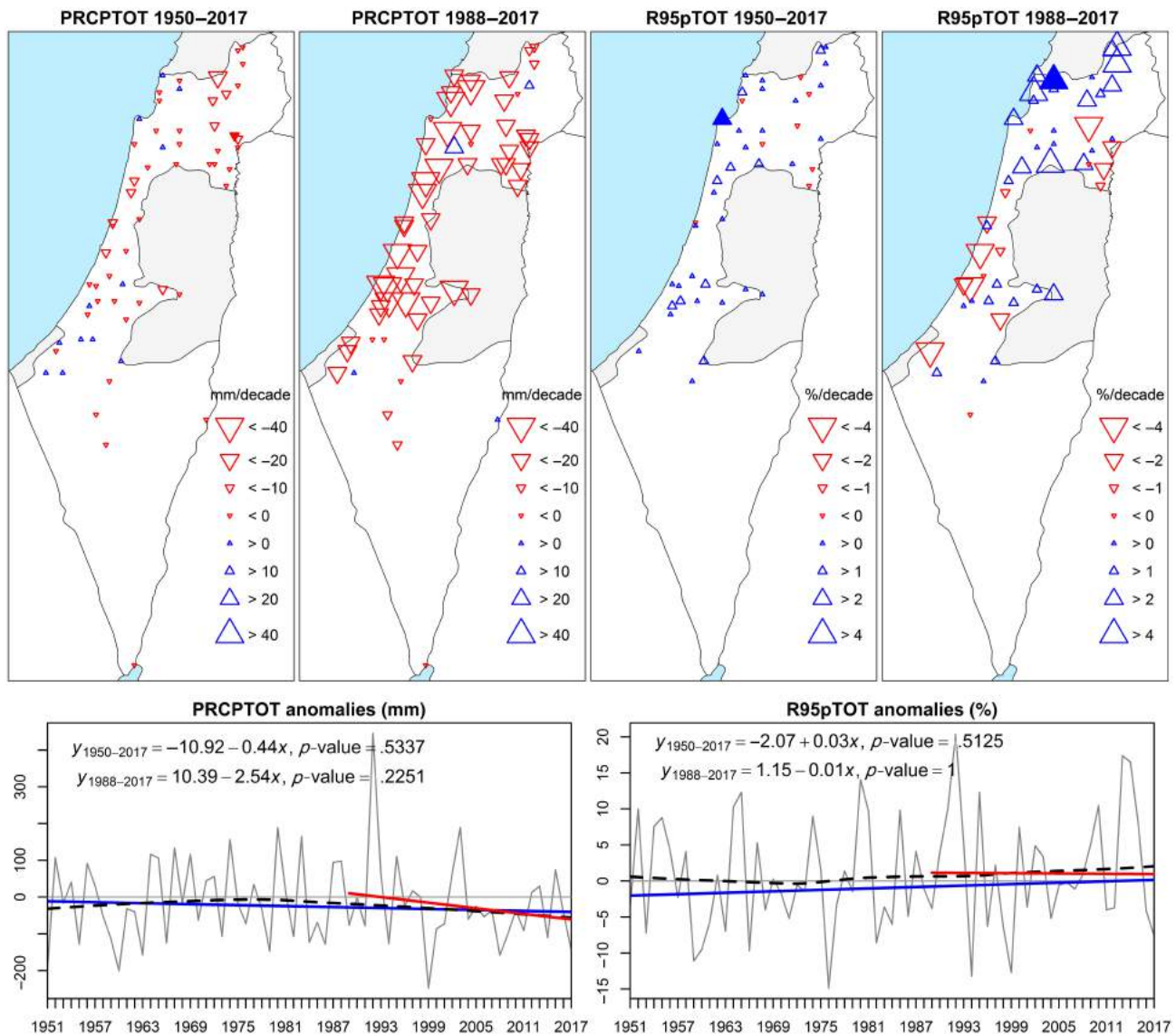


FIGURE 14 Trend in the PRCPTOT and in the contribution from very wet days (R95pTOT) for the period 1950–2017 and 1988–2017. Upward blue triangles represent increasing trends, and downward red triangles represent decreasing trends. Different sized triangles indicate different magnitudes of trends. Significant changes ($p \leq .05$) are indicated by filled triangles. (unit: mm/decade; %/decade, respectively) [Colour figure can be viewed at wileyonlinelibrary.com]

be attributed to the fact that the number of events with at least six consecutive days when $TN < 10$ th percentile (CSDI) are very rare. Therefore, the ET-SCI CSDI3 (at least three consecutive days when $TN < 10$ th) index was added to the analysis.

Generally, significantly increasing trends in the number of warm days and nights along with decreasing trends of number of cold days and nights were found for both periods 1950–2017 and 1988–2017. On one hand, our findings are consistent with Zhang *et al.* (2005a), although their study lacked spatial long representation of our region (Israel, Jordan, Syria, Lebanon) due to lack of data availability from the 1950s. On the other hand, we have found more intense rates for the TX90p, TN90p and WSDI over the last

30 years. Since the 1990s, the latter indices have increased sharply, continuing to break more temperature records, leading to much stronger upwards trends, 14 years after Zhang *et al.*'s (2005a) comprehensive study ended.

Note that percentile-based indices are much more sensitive to the selected reference period compared to the others. When using different reference periods, the magnitude of the trends may change, depending upon whether percentiles are derived from a relatively colder or warmer reference period. Based on several sensitivity tests, we have conducted, it was found that percentiles from the reference period 1961–1990 and 1971–2000 exhibit a similar trend magnitude, unlike those derived from much warmer periods, such as in

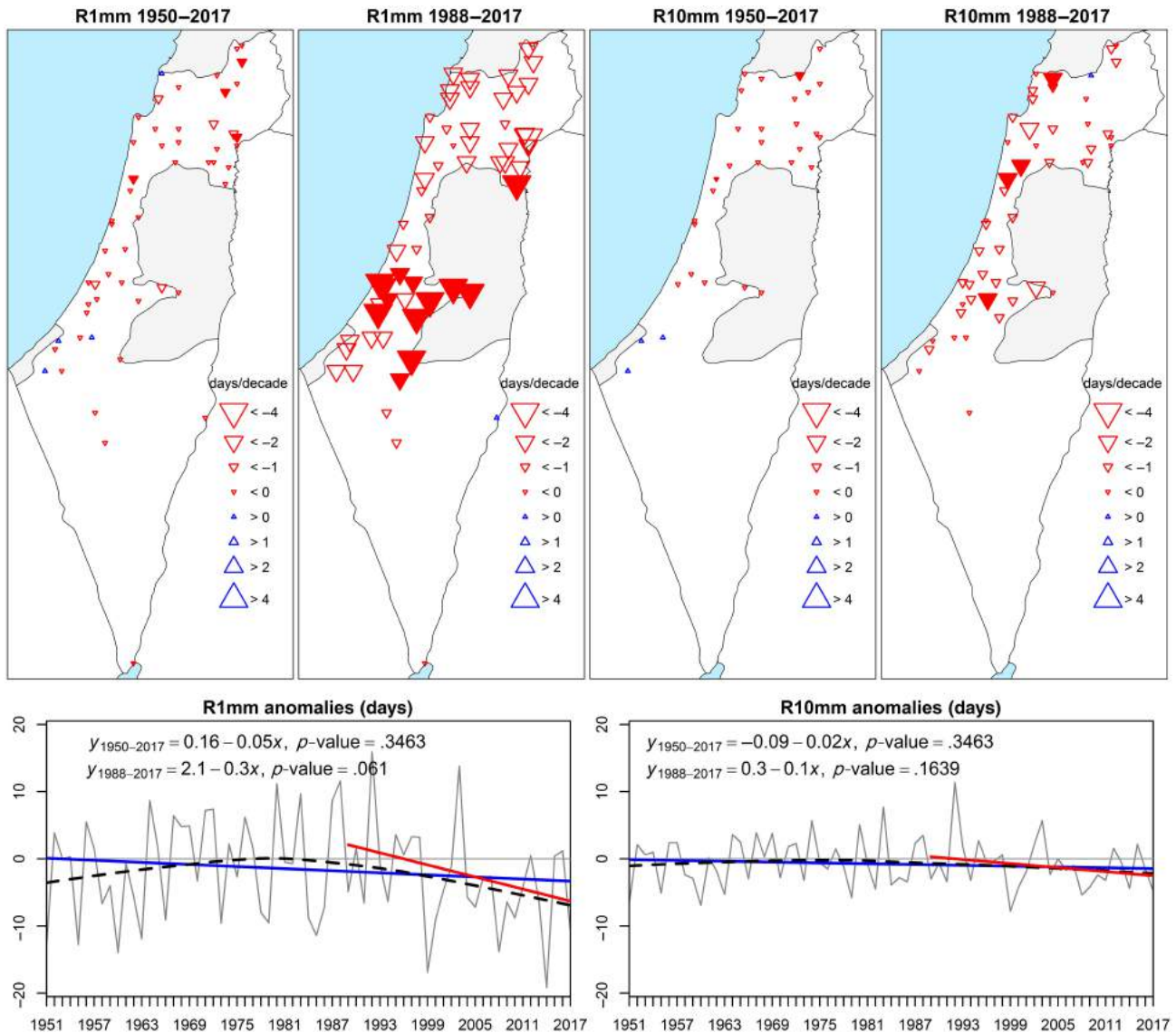


FIGURE 15 Trend in the annual amount of wet days when precipitation ≥ 1 mm (R1mm, left panel) and precipitation ≥ 10 mm (R10mm, right panel) for 1950–2017 and 1988–2017 (unit: days/decade). The symbols for the maps are the same as Figure 14 and the graphs as Figure 5 [Colour figure can be viewed at wileyonlinelibrary.com]

1981–2010. Consequently, the trend magnitude of the cold day/night indices is amplified, while the trend magnitude of the warm day/night is diminished when using a warmer reference period for the EM region. These features are even more pronounced during the last 30 years. Figure 17 shows an example of this feature for TN10p and TX90p.

The absolute temperature indices (TXx, TXn, TNx, TNn) show a general warming trend, while only the highest minimum temperature (TNx, warmest night) shows a significant increasing trend that has more than doubled over the last 30 years. Zhang *et al.* (2005a) found similar tendencies for the ME but with statistically significant trends for all the four indices over 1970–2003. Note that these four indices represent only one value per year at the very upper tail of the distributions, and is therefore

based on a much smaller sample, undergoing higher variability compared to the indices that typically occur several times per year. Moreover, the interannual variability in the TNx (usually measured during the summer) is smaller than that of the annual TXx, TXn and TNn, reflecting much smaller variability in the summer than in the winter. As a consequence, the winter season is more challenging for significant trend detection, due to the low signal-to-noise ratio.

Changes in precipitation are characterized by higher spatial and temporal variability than temperature. The annual precipitation trends (positive and negative) for all the indices were found to be not statistically significant for both periods 1950–2017 and 1988–2017. These non-significant precipitation trends are in accordance with other studies for the ME

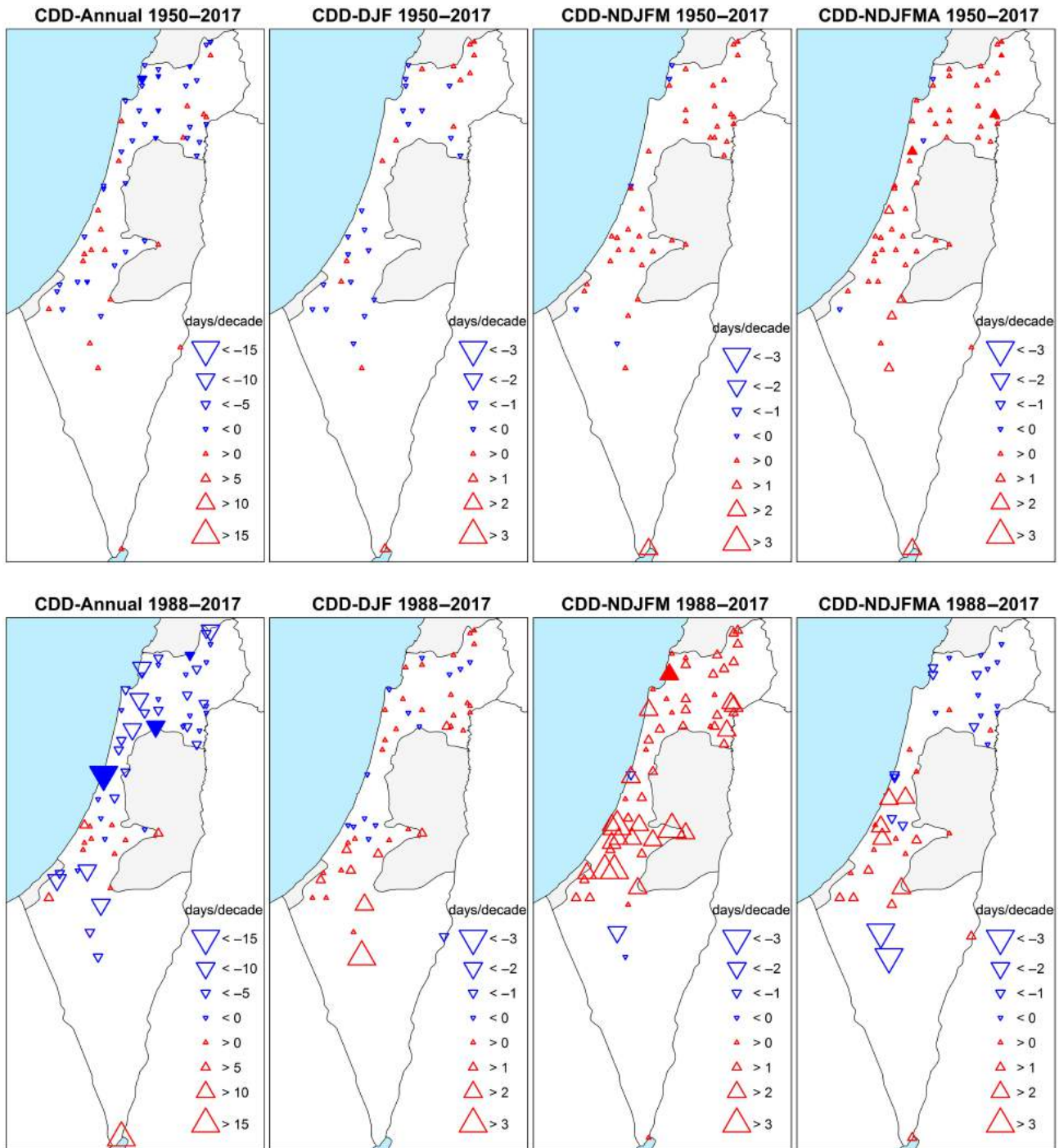


FIGURE 16 Same as Figure 8 except for different periods of CDD index: Annual, DJF, NDJFM and NDJFMA (unit: days/decade) [Colour figure can be viewed at wileyonlinelibrary.com]

(e.g., Alpert *et al.*, 2002; Zhang *et al.*, 2005a; Yosef *et al.*, 2009; AlSarmi and Washington, 2011; Shohami *et al.*, 2011).

Morin (2011) suggests that a relatively high magnitude of trends of precipitation data have low probability of being detected, as a result of the high natural variance of precipitation data. Hence, the probability of significant trend detection is a function of signal-to-noise ratio and the record length. Followed by Morin (2011), Shohami *et al.* (2011) argued that

the insignificant trends for the precipitation series may be interpreted as potential change that is not yet large enough to be detected, rather than no change at all. Frei and Schär (2001) stressed that “*The absence of statistical significance is not synonymous to the absence of trends in the data*” since substantial long-term changes can be masked by the stochastic fluctuations. They showed that the potential to detect a trend is expressed in terms of probability determined as a function

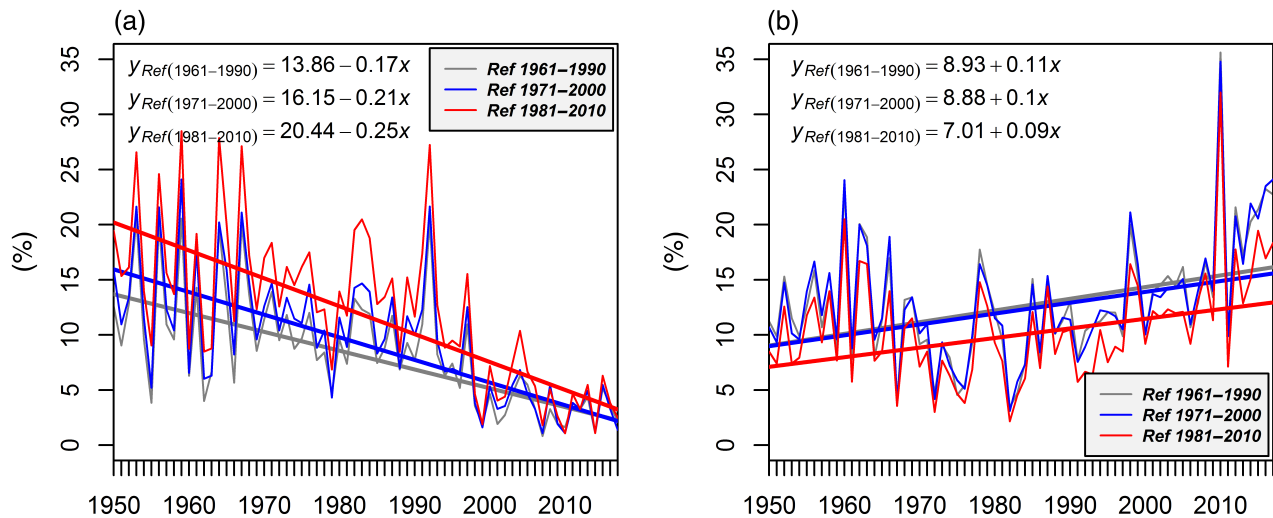


FIGURE 17 The linear trends of (a) TN10p and (b) TX90p when percentiles derived from different reference periods: 1961–1990 (grey), 1971–2000 (blue) and 1981–2010 (red). Example is shown from Jerusalem records [Colour figure can be viewed at wileyonlinelibrary.com]

of the record length, the magnitude of the trend, and the rarity of events, for precipitation in the Alpine region.

A reduction in the total precipitation amount, together with its tendency towards a higher contribution from very wet days (R95pTOT), was found. These opposite trends have been more pronounced during the last 30 years, when the northern part of the country has been characterized by more intense wet days along with drier conditions. This is consistent with our reported pattern for RX5days index as well. A similar feature was found for the centre of the country, followed by weaker trends and a statistically significant decrease in the number of wet days (R1mm). This general (non-significant) tendency of decreases in total rainfall amount in spite of an increase in extreme daily rainfall in Israel is in agreement with Alpert *et al.* (2002) and with Yosef *et al.* (2009) who described a regional increase in percentage from the total annual amounts of “Moderate-Heavy” (16–32 mm/day) and “Heavy” (32–64 mm/day) categories for the north and the centre of Israel, respectively, over 1950/1–2003/4. Moreover, the spatial CDD-NDJFMA distribution (i.e., the whole rainy season) showed downward tendencies for the north during the last 30 years (Figure 16), while the long-term trend showed upward tendencies that were more pronounced during the short-term CDD-NDJFM. The latter is in agreement with Ziv *et al.* (2014) who reported on a lengthening trend in the dry spells between November and March, over Israel for 1975–2010.

Part of the reduction in the total precipitation amount over the EM can be attributed to changes in large atmospheric circulation. For instance, due to expansion of the Hadley Cell towards the Poles (Fu *et al.*, 2006; Lu *et al.*, 2007), the subtropical dry zones also expand poleward. Givati and Rosenfeld (2013) have shown that a trend of increasing Arctic Oscillation is associated with a substantial

decrease of winter precipitation from the Iberian Peninsula, through Italy, Greece, Turkey, Cyprus, Lebanon, Syria and also the northern parts of Israel. Regarding extreme precipitation events over EM, Toreti *et al.* (2010b) identified anomaly circulation patterns that suggest warm advection associated with anomalous ascent motions and an increase of low to mid tropospheric moisture. Moreover, they pointed out that the subtropical jet stream with its axis oriented South-West/North-East (where maximum velocity is located over Egypt) supports the eastern basin being situated in a divergence area, where ascent motions are favoured. These findings are in accordance with Dayan *et al.* (2001) who analysed a specific severe autumn storm over ME. Shohami *et al.* (2011) reported changes in atmospheric conditions (e.g., pressure from sea level up to the tropopause, downward vertical motion at 500 hPa and humidity at 700 hPa) during winter, and the transitional seasons support drier conditions due to reduction in cyclogenesis and specific humidity over the EM.

Recently, a new study (Hochman *et al.*, 2018) projected changes for the extreme temperature and precipitation indices (2041–2070), at a very high resolution (about 8 km) over the region of Israel. A pronounced increase in the mean temperature was predicted (mainly in autumn and winter), while the extreme temperature indices projected larger increase in the minimum temperature than the maximum. Regarding precipitation, decreases are projected for the north and the centre. These findings are in accordance with the previously described climatic changes in this study. As opposed to the projection made by Hochman *et al.* (2018), we have found a decreasing rather than increasing trend in the annual CDD. Furthermore, the rise of the mean temperature is mainly attributed to the summer (at least for the moment) rather than the autumn or winter.

5 | SUMMARY AND CONCLUSIONS

For the first time, long Israeli daily time series have undergone a homogenization procedure that involved adjustments for site relocations, instruments changes, different screen types, etc. The analysis was done for 38 temperature (TX and TN) stations and 60 precipitation stations for the period 1950–2017. Thus we present a new ground station dataset of climate extreme indices based on novel homogenized daily temperature and precipitation records. To the best of our knowledge, this is the most comprehensive study using long daily records gathered from dense ground meteorological stations (high spatial resolution) conducted in our region.

The study examines 38 extreme temperature and precipitation indices developed by ETCCDI and ET-SCI (few indices were modified by the authors). Since we used the internationally coordinated exact formula for each index, the present analyses for Israel fit seamlessly together with analyses in the other regions where a similar analysis has already been done.

The time series were pre-whitened (Wang and Swail, 2001), while the trends and their significance level were calculated using the robust non-parametric Mann–Kendall test (Mann, 1945; Kendall, 1955) and the Sen's slope estimator (Sen, 1968).

The main findings of this study are as follows:

1. Almost all the temperature time series were found to be inhomogeneous, stressing that homogenization is an essential part in the analysis; otherwise misleading interpretations/conclusions about climate change might be reached.
2. Highly significant, spatially coherent warming trends were observed for 1950–2017 that became more pronounced over the period 1988–2017. We have found downward trends from the 1950s until the 1970s, followed by sharp upward trends since the beginning of the 1990s onwards, revealing non-monotonic trends.
3. For the last 30 years, the annual TX and TN showed similar increasing magnitudes ($\sim 0.55^\circ\text{C}/\text{decade}$), when for the same period a significant increase was detected in the winter for both parameters (0.7 and $0.4^\circ\text{C}/\text{decade}$, respectively). Still, the summer and spring lead the long- and short-term warming trends.
4. Significant warming trends related to temperature extreme indices, mostly stronger for indices based on daily TN than for indices calculated from daily TX. The highest increase was found for the summer extreme indices (e.g., TX90p, TN90p, TNx).
5. Significant increasing trends in the number of warm nights and days along with a decrease in number of cold nights and days were found for both study periods.

The coastal area tends to exhibit more intense heat stress during the night together with strong increasing temperatures over the mountains around noon.

6. Warm spell duration significantly increases while cold spell duration shows a weaker decreasing tendency, which is not statistically significant for 1988–2017.
7. The regional and the local precipitation changes show mostly statistically non-significant (decreasing/increasing) trends although exhibiting satisfactory spatial coherency.
8. A reduction in the total precipitation amount along with a tendency towards a higher contribution from very wet days is much stronger for the last 30 years (statistically not significant).
9. Decreasing long-term trends in the annual CDD and CDD-DJF indices were found, with the exception of the northern tip of the country, where weak increasing trends for CDD-DJF were noted for both periods.
10. It is likely that precipitation trends are masked due to strong temporal variability (signal-to-noise ratio issue) along with the study period length and the trend magnitude that makes this difficult to detect.

This study not only contributes to our understanding of changes in climate extremes, but also provides a long-term homogenized dataset for a region that suffers from a deficiency of long reliable time series. Considering the urgency for more climate change studies in the EM, these findings provide important insights for future research.

ACKNOWLEDGEMENTS

The authors are indebted to the Climate Department of the IMS for providing the data and the metadata for this study. Noam Halfon was especially helpful to us in creating Figure 1 maps and participating in fruitful discussions. The authors would also like to thank the Israeli Science Foundation (grant number 1123/17).

ORCID

Yizhak Yosef  <https://orcid.org/0000-0002-3010-3188>

REFERENCES

- Aguilar, E., Auer, I., Brunet, M., Peterson, T.C. and Wieringa, J. (2003) *Guidelines on climate metadata and homogenisation*. Geneva: World Meteorological Organization. WCDMP-No. 53, WMO-TD No. 1186.
- Alexander, L. and Herold, N. (2015) *ClimPACTv2 Indices and Software. A Document Prepared on Behalf of the Commission for Climatology (CCI) Expert Team on Sector-Specific Climate Indices (ET-SCI)*. Sydney.

- Alexandersson, H. (1986) A homogeneity test applied to precipitation data. *Journal of Climatology*, 6(6), 661–675.
- Alpert, P., Ben-Gai, T., Baharad, A., Benjamini, Y., Yekutieli, D., Colacino, M., Diodato, L., Ramis, C., Homar, V., Romero, R. and Michaelides, S. (2002) The paradoxical increase of Mediterranean extreme daily rainfall in spite of decrease in total values. *Geophysical Research Letters*, 29(11), 31–31.
- Alpert, P., Krichak, S.O., Shafir, H., Haim, D. and Osetinsky, I. (2008) Climatic trends to extremes employing regional modeling and statistical interpretation over the E. Mediterranean. *Global and Planetary Change*, 63(2), 163–170.
- AlSarmi, S. and Washington, R. (2011) Recent observed climate change over the Arabian Peninsula. *Journal of Geophysical Research: Atmospheres*, 116(D11).
- Barry, A.A., Caesar, J., Klein Tank, A.M.G., Aguilar, E., McSweeney, C., Cyrille, A.M., Nikiema, M.P., Narcisse, K.B., Sima, F., Stafford, G. and Touray, L.M. (2018) West Africa climate extremes and climate change indices. *International Journal of Climatology*, 38, e921–e938.
- Ben-Gai, T., Bitan, A., Manes, A., Alpert, P. and Rubin, S. (1999) Temporal and spatial trends of temperature patterns in Israel. *Theoretical and Applied Climatology*, 64, 163–177.
- Bronaugh, D. and Werner, A. (2013) *zyp: Zhang + Yue-Pilon trends package*. R package version, 0.10-1. Available at: <http://CRAN.R-project.org/package=zyp> [Accessed 20th January, 2019].
- Brunetti, M., Maugeri, M., Monti, F. and Nanni, T. (2006) Temperature and precipitation variability in Italy in the last two centuries from homogenised instrumental time series. *International Journal of Climatology: A Journal of the Royal Meteorological Society*, 26(3), 345–381.
- Caussinus, H. and Mestre, O. (2004) Detection and correction of artificial shifts in climate series. *Journal of the Royal Statistical Society: Series C (Applied Statistics)*, 53(3), 405–425.
- Cleveland, W.S. (1979) Robust locally weighted regression and smoothing scatterplots. *Journal of the American Statistical Association*, 74(368), 829–836.
- Close, B. and Zurbenko, I. (2016) *kza: Kolmogorov-Zurbenko adaptive filters*. R package version 4.0.0. Available at: <http://CRAN.R-project.org/package=kza> [Accessed 20th January, 2019].
- Dayan, U., Ziv, B., Margalit, A., Morin, E. and Sharon, D. (2001) A severe autumn storm over the Middle-East: synoptic and mesoscale convection analysis. *Theoretical and Applied Climatology*, 69 (1–2), 103–122.
- Della-Marta, P.M. and Wanner, H. (2006) A method of homogenizing the extremes and mean of daily temperature measurements. *Journal of Climate*, 19(17), 4179–4197.
- Domonkos, P. (2011) Adapted Caussinus-Mestre algorithm for networks of temperature series (ACMANT). *International Journal of Geosciences*, 2(3), 293–309.
- Domonkos, P. and Coll, J. (2017) Homogenisation of temperature and precipitation time series with ACMANT3: method description and efficiency tests. *International Journal of Climatology*, 37(4), 1910–1921.
- Domroes, M. and El-Tantawi, A. (2005) Recent temporal and spatial temperature changes in Egypt. *International Journal of Climatology: A Journal of the Royal Meteorological Society*, 25(1), 51–63.
- Donat, M.G. and Alexander, L.V. (2012) The shifting probability distribution of global daytime and night-time temperatures. *Geophysical Research Letters*, 39(14).
- Donat, M.G., Alexander, L.V., Yang, H., Durre, I., Vose, R., Dunn, R., J.H., Willett, K.M., Aguilar, E., Brunet, M., Caesar, J., Hewitson, B., Jack, C., Tank, A.M.K., Kruger, A.C., Marengo, J., Peterson, T.C., Renom, M., Rojas, C.O., Rusticucci, M., Salinger, J., Elrayah, A.S., Sekele, S.S., Srivastava, A.K., Trewin, B., Villarreal, C., Vincent, L.A., Zhai, P., Zhang, X. and Kitching, S. (2013) Updated analyses of temperature and precipitation extreme indices since the beginning of the twentieth century: the HadEX2 dataset. *Journal of Geophysical Research: Atmospheres*, 118, 2098–2118. <https://doi.org/10.1002/jgrd.50150>.
- Easterling, D.R., Horton, B., Jones, P.D., Peterson, T.C., Karl, T.R., Parker, D.E., Salinger, M.J., Razuvayev, V., Plummer, N., Jamason, P. and Folland, C.K. (1997) Maximum and minimum temperature trends for the globe. *Science*, 277(5324), 364–367.
- Frei, C. and Schär, C. (2001) Detection probability of trends in rare events: theory and application to heavy precipitation in the Alpine region. *Journal of Climate*, 14(7), 1568–1584.
- Fu, Q., Johanson, C.M., Wallace, J.M. and Reichler, T. (2006) Enhanced mid-latitude tropospheric warming in satellite measurements. *Science*, 312(5777), 1179–1179.
- Givati, A. and Rosenfeld, D. (2013) The Arctic Oscillation, climate change and the effects on precipitation in Israel. *Atmospheric Research*, 132, 114–124.
- Guijarro, J.A. (2011) *User's Guide to Climatol. An R Contributed Package for Homogenization of Climatological Series*. Spain: State Meteorological Agency, Balearic Islands Office.
- Guijarro, J.A. (2018) *Homogenization of Climatic Series with Climatol*. Spain: State Meteorological Agency (AEMET), Balearic Islands Office.
- Hochman, A., Mercogliano, P., Alpert, P., Saaroni, H. and Bucchignani, E. (2018) High-resolution projection of climate change and extremity over Israel using COSMO-CLM. *International Journal of Climatology*, 38(14), 5095–5106.
- IPCC. (2014) *Climate Change 2014: Synthesis Report. Contribution of Working Groups I, II and III to the Fifth Assessment Report of the Intergovernmental Panel on Climate Change* [Core Writing Team, Pachauri, R.K. and Meyer, L.A. (Eds.)]. Geneva: IPCC.
- Jones, P.D. and Hulme, M. (1996) Calculating regional climatic time series for temperature and precipitation: methods and illustrations. *International Journal of Climatology*, 16(4), 361–377.
- Kendall, M.G. (1955) *Rank Correlation Methods*. London: Charles Griffin, p. 196.
- Klein Tank, A.M.G., Peterson, T.C., Quadir, D.A., Dorji, S., Zou, X., Tang, H., Santhosh, K., Joshi, U.R., Jaswal, A.K., Kolli, R.K. and Sikder, A.B. (2006) Changes in daily temperature and precipitation extremes in central and South Asia. *Journal of Geophysical Research: Atmospheres*, (D16), 111.
- Klein Tank, A. M. G., Zwiers, F. W. and Zhang, X. (2009) *Guidelines on analysis of extremes in a changing climate in support of informed decisions for adaptation. Climate data and monitoring*. Geneva: World Meteorological Organization. WCDMP-No. 72, WMO-TD No.1500.
- Kostopoulou, E. and Jones, P.D. (2005) Assessment of climate extremes in the Eastern Mediterranean. *Meteorology and Atmospheric Physics*, 89(1–4), 69–85.
- Leduc, D.J. (1987) A comparative analysis of the reduced major axis technique of fitting lines to bivariate data. *Canadian Journal of Forest Research*, 17, 654–659.

- Lu, J., Vecchi, G.A. and Reichler, T. (2007) Expansion of the Hadley cell under global warming. *Geophysical Research Letters*, (6), 34.
- Mamara, A., Argiriou, A.A. and Anadranistakis, M. (2016) Recent trend analysis of mean air temperature in Greece based on homogenized data. *Theoretical and Applied Climatology*, 126(3–4), 543–573.
- Mann, H.B. (1945) Non-parametric tests against trend. *Econometrica*, 13, 245–259.
- Mariotti, A., Pan, Y., Zeng, N. and Alessandri, A. (2015) Long-term climate change in the Mediterranean region in the midst of decadal variability. *Climate Dynamics*, 44(5–6), 1437–1456.
- Mestre, O., Domonkos, P., Picard, F., Auer, I., Robin, S., Lebarbier, E., Böhm, R., Aguilar, E., Guijarro, J., Vertachnik, G. and Klancar, M. (2013) HOMER: a homogenization software—methods and applications. *Időjárás-Quarterly Journal of the Hungarian Meteorological Service*, 117(1), 47–67.
- Mestre, O., Gruber, C., Prieur, C., Caussin, H. and Jourdain, S. (2011) SPLIDHOM: a method for homogenization of daily temperature observations. *Journal of Applied Meteorology and Climatology*, 50(11), 2343–2358.
- Morin, E. (2011) To know what we cannot know: global mapping of minimal detectable absolute trends in annual precipitation. *Water Resources Research*, 47(7).
- Pettit, A.N. (1979) A non-parametric approach to the changepoint problem. *Applied Statistics*, 28, 126–135.
- Picard, F., Lebarbier, E., Hoebeke, M., Rigail, G., Thiam, B. and Robin, S. (2011) Joint segmentation, calling, and normalization of multiple CGH profiles. *Biostatistics*, 12(3), 413–428.
- Price, C., Michaelides, S., Pashiardis, S. and Alpert, P. (1999) Long term changes in diurnal temperature range in Cyprus. *Atmospheric Research*, 51(2), 85–98.
- Saaroni, H., Ziv, B., Edelson, J. and Alpert, P. (2003) Long-term variations in summer temperatures over the Eastern Mediterranean. *Geophysical Research Letters*, 30(18).
- Saaroni, H., Ziv, B., Osetinsky, I. and Alpert, P. (2010) Factors governing the interannual variation and the long-term trend of the 850 hPa temperature over Israel. *Quarterly Journal of the Royal Meteorological Society*, 136(647), 305–318.
- Sen, P.K. (1968) Estimates of the regression coefficient based on Kendall's tau. *Journal of the American Statistical Association*, 63, 1379–1389.
- Shohami, D., Dayan, U. and Morin, E. (2011) Warming and drying of the eastern Mediterranean: additional evidence from trend analysis. *Journal of Geophysical Research: Atmospheres*, 116(D22).
- Tanarhte, M., Hadjinicolaou, P. and Lelieveld, J. (2012) Intercomparison of temperature and precipitation data sets based on observations in the Mediterranean and the Middle East. *Journal of Geophysical Research: Atmospheres*, 117(D12).
- Thorne, P.W., Donat, M.G., Dunn, R.J.H., Williams, C.N., Alexander, L.V., Caesar, J., Durre, I., Harris, I., Hausfather, Z., Jones, P.D. and Menne, M.J. (2016) Reassessing changes in diurnal temperature range: intercomparison and evaluation of existing global data set estimates. *Journal of Geophysical Research: Atmospheres*, 121(10), 5138–5158.
- Toreti, A., Fioravanti, G., Perconti, W. and Desiato, F. (2009) Annual and seasonal precipitation over Italy from 1961 to 2006. *International Journal of Climatology: A Journal of the Royal Meteorological Society*, 29(13), 1976–1987.
- Toreti, A., Kuglitsch, F.G., Xoplaki, E., Luterbacher, J. and Wanner, H. (2010a) A novel method for the homogenization of daily temperature series and its relevance for climate change analysis. *Journal of Climate*, 23(19), 5325–5331.
- Toreti, A., Xoplaki, E., Maraun, D., Kuglitsch, F.G., Wanner, H. and Luterbacher, J. (2010b) Characterisation of extreme winter precipitation in Mediterranean coastal sites and associated anomalous atmospheric circulation patterns. *Natural Hazards and Earth System Sciences*, 10(5), 1037–1050.
- Trewin, B. (2013) A daily homogenized temperature data set for Australia. *International Journal of Climatology*, 33(6), 1510–1529.
- Venema, V.K.C., Mestre, O., Aguilar, E., Auer, I., Guijarro, J.A., Domonkos, P., Vertachnik, G., Szentimrey, T., Stepanek, P., Zahradnicek, P., Viarre, J., Mller-Westermeier, G., Lakatos, M., Williams, C.N., Menne, M.J., Lindau, R., Rasol, D., Rustemeier, E., Kolokythas, K., Marinova, T., Andresen, L., Acquafatta, F., Fratianni, S., Cheval, S., Klancar, M., Brunetti, M., Gruber, C., Prohom Duran, M., Likso, T., Esteban, P. and Brandsma, T. (2012) Benchmarking homogenization algorithms for monthly data. *Climate of the Past*, 8, 89–115. <https://doi.org/10.5194/cp-8-89-2012>.
- Vincent, L.A., Wang, X.L., Milewska, E.J., Wan, H., Yang, F. and Swail, V. (2012) A second generation of homogenized Canadian monthly surface air temperature for climate trend analysis. *Journal of Geophysical Research: Atmospheres*, 117(D18).
- Vincent, L.A., Zhang, X., Bonsal, B.R. and Hogg, W.D. (2002) Homogenization of daily temperatures over Canada. *Journal of Climate*, 15(11), 1322–1334.
- Wang, X.L. (2008) Accounting for autocorrelation in detecting mean shifts in climate data series using the penalized maximal t or F test. *Journal of Applied Meteorology and Climatology*, 47(9), 2423–2444.
- Wang, X.L. and Feng, Y. (2013) *RHtestsV4 User Manual*. Toronto: Climate Research Division, Atmospheric Science and Technology Directorate, Science and Technology Branch, Environment Canada.
- Wang, X.L. and Swail, V.R. (2001) Changes of extreme wave heights in Northern Hemisphere oceans and related atmospheric circulation regimes. *Journal of Climate*, 14, 2204–2220.
- Yosef, Y., Aguilar, E. and Alpert, P. (2018) Detecting and adjusting artificial biases of long-term temperature records in Israel. *International Journal of Climatology*, 38(8), 3273–3289.
- Yosef, Y., Saaroni, H. and Alpert, P. (2009) Trends in daily rainfall intensity over Israel 1950/1–2003/4. *Open Atmospheric Science Journal*, 3, 196–203.
- Ziv, B., Saaroni, H., Baharad, A., Yekutieli, D. and Alpert, P. (2005) Indications for aggravation in summer heat conditions over the Mediterranean Basin. *Geophysical Research Letters*, 32, L12706. <https://doi.org/10.1029/2005GL022796>.
- Ziv, B., Saaroni, H., Pargament, R., Harpaz, T. and Alpert, P. (2014) Trends in rainfall regime over Israel, 1975–2010, and their relationship to large-scale variability. *Regional Environmental Change*, 14(5), 1751–1764.
- Zhang, X., Aguilar, E., Sensoy, S., Melkonyan, H., Tagiyeva, U., Ahmed, N., Kutsaladze, N., Rahimzadeh, F., Taghipour, A., Hantosh, T.H. and Alpert, P. (2005a) Trends in Middle East climate extreme indices from 1950 to 2003. *Journal of Geophysical Research: Atmospheres*, 110(D22).
- Zhang, X., Alexander, L., Hegerl, G.C., Jones, P., Tank, A.K., Peterson, T.C., Trewin, B. and Zwiers, F.W. (2011) Indices for

- monitoring changes in extremes based on daily temperature and precipitation data. *Wiley Interdisciplinary Reviews: Climate Change*, 2(6), 851–870.
- Zhang, X., Hegerl, G., Zwiers, F.W. and Kenyon, J. (2005b) Avoiding inhomogeneity in percentile-based indices of temperature extremes. *Journal of Climate*, 18(11), 1641–1651.
- Zhang, X., Vincent, L.A., Hogg, W.D. and Niitsoo, A. (2000) Temperature and precipitation trends in Canada during the 20th century. *Atmosphere-Ocean*, 38(3), 395–429.
- Zhang, X. and Yang, F. (2004) *RClimDex (1.0) User Guide*. Ontario: Climate Research Branch Environment Canada.
- Zurbenko, I., Porter, P.S., Gui, R., Rao, S.T., Ku, J.Y. and Eskridge, R. E. (1996) Detecting discontinuities in time series of upper-air data: development and demonstration of an adaptive filter technique. *Journal of Climate*, 9(12), 3548–3560.
- Zurbenko, I.G. and Sun, M. (2017) Applying Kolmogorov-Zurbenko adaptive R-software. *International Journal of Statistics and Probability*, 6(5), 110.
- Zwiers, F.W., Alexander, L.V., Hegerl, G.C., Knutson, T.R., Kossin, J.P., Naveau, P., Nicholls, N., Schär, C., Seneviratne, S.

I. and Zhang, X. (2013) Climate extremes: challenges in estimating and understanding recent changes in the frequency and intensity of extreme climate and weather events. In: Asrar, G.R. and Hurrell, J.W. (Eds.) *Climate Science for Serving Society: Research, Modeling and Prediction Priorities*. Dordrecht: Springer, pp. 339–389.

SUPPORTING INFORMATION

Additional supporting information may be found online in the Supporting Information section at the end of this article.

How to cite this article: Yosef Y, Aguilar E, Alpert P. Changes in extreme temperature and precipitation indices: Using an innovative daily homogenized database in Israel. *Int J Climatol*. 2019; 1–24. <https://doi.org/10.1002/joc.6125>